Computational Fluid Dynamics (CFD) and Thermal Analysis for Kettle Reboiler

Master of Engineering

In

(Thermal Engineering)

Prashant Panwar

Roll no.: 802383003

Under the supervision of

Sandeep Goyal
(Head Of the Department)
ISGEC Heavy Engineering LTD., Yamuna Nagar

Dr. Gautam Setia
(Assistant Professor)
Mechanical Engineering Department
Thapar Institute of Engineering and Technology, Patiala

Nitish Kumar
(Deputy Manager)
ISGEC Heavy Engineering LTD., Yamuna Nagar

Dr. Sayan Sadhu
(Assistant Professor)
Mechanical Engineering Department
Thapar Institute of Engineering and Technology, Patiala

MECHANICAL ENGINEERING DEPARTMENT

THAPAR INSTITUTE OF ENGINEERING & TECHNOLOGY PATIALA

(August 2025)

DECLARATION

I, **Prashant Panwar**, solemnly declare that the research work titled **"Computational Fluid Dynamics (CFD) and Thermal Analysis for Kettle Reboiler"** is an original contribution carried out by me during my major project at **ISGEC Heavy Engineering Ltd., Yamuna Nagar**, in collaboration with **Thapar Institute of Engineering and Technology, Patiala**.

This project was conducted under the expert guidance of my mentors: **Mr. Nitish Kumar, Mr. Sandeep Goyal, Dr. Sayan Sadhu, and Dr. Gautam Setia**. I affirm that the work presented in this study is my own and has not been submitted elsewhere for any academic degree or certification.

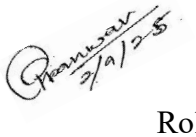

Prashant Panwar

Roll No. 802383003

I certify that the above statement made by the student is accurate to the best of my knowledge and belief.

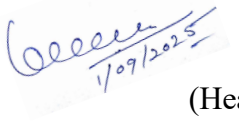

Sandeep Goyal
(Head Of the Department)
ISGEC Heavy Engineering LTD., Yamuna Nagar

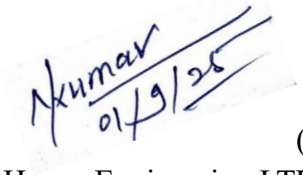

Nitish Kumar
(Deputy Manager)
ISGEC Heavy Engineering LTD., Yamuna Nagar

Dr. Gautam Setia
(Assistant Professor)
Mechanical Engineering Department
Thapar Institute of Engineering and Technology, Patiala

Dr. Sayan Sadhu
(Assistant Professor)
Mechanical Engineering Department
Thapar Institute of Engineering and Technology, Patiala

ACKNOWLEDGEMENTS

The successful completion of this project would not have been possible without the invaluable guidance, supervision, and support I received throughout my research. I am truly thankful to each person who supported this project.

First and foremost, I would like to express my sincere gratitude to my thesis supervisors, Mr. Nitish Kumar, Mr. Sandeep Goyal, Dr. Gautam Setia, and Dr. Sayan Sadhu, for their expert guidance and encouragement. Their insightful feedback, constant motivation, and constructive criticism played a pivotal role in shaping this project from inception to completion. I am particularly thankful for their patience and willingness to guide me, even amidst their busy schedules.

I would also like to extend my special thanks to **Dr. Rajesh Shukla** for his crucial assistance in setting up and troubleshooting **ANSYS**, which was an essential part of my computational analysis. His expertise and timely support were instrumental in overcoming technical challenges.

Additionally, I am grateful to the faculty members of the **Mechanical Engineering Department** for their unwavering support and encouragement throughout my academic journey. The combined expertise and advice they provided proved essential to my educational growth.

Lastly, I appreciate the collaborative and friendly work environment that made this project a rewarding experience.

Prashant Panwar

Roll No. 802383003

Thapar Institute of Engineering and Technology, Patiala

Table Of Contents

Section	Page No.
Declaration	2
Acknowledgements	3
Table of Contents	4
List of Figures	6
List of Tables	7
Nomenclature	8
Abstract	9
Chapter 1: Introduction	10
1.1 Background	10
1.2 Classification of Heat Exchangers	10
1.3 Schematic Illustration of Construction	15
1.4 Kettle Reboilers and Vaporizers	15
1.4.1 Reboiler Selection	17
Chapter 2: Literature Review	18
2.1 Literature Summary	18
2.2 Research Gap	19
2.3 Research Objective	20
Chapter 3: Methodology	21
3.1 Problem Statement	21
3.2 Numerical Simulation	22
3.2.1 Geometry Modeling	22
3.2.2 Mesh Modeling	23
3.3 Physics	24
3.3.1 Model	24
3.3.2 Material Properties	24
3.3.3 Cell Zone Conditions	26
3.3.4 Boundary Conditions	27
3.3.5 Solver Settings	30
Chapter 4: Results and Discussion	32
4.1 Case 1: Dia 1790 mm	32
4.1.1–4.1.5 (Pressure, Temp, etc.)	32
4.2 Case 2: Dia 1750 mm	34
4.3 Case 3: Dia 1690 mm	37

4.4 Discussion 38
4.5 Comparison 39
4.6 Cost Estimation 39
Chapter 5: Conclusion and Future Scope 41
5.1 Conclusion 41
5.2 Future Scope 41
References 42

List of Figures

Figure No.	Title	Page No.
Fig-1.1	Classification Of Heat Exchangers. [1]	11
Fig-1.2	(A) Classification According to Process Function. (B) Classification Of Condensers. (C) Classification Of Liquid-To-Vapor Phase-Change Exchangers. [2]	12
Fig-1.3	Standard Front-End Head, Shell-Type, And Rear-End Head Types, From Tema [5]	13
Fig-1.4	Schematic Illustration of Shell-And-Tube Heat Exchanger Construction [8]	14
Fig-1.5	Tema K-Type Shell. [5]	14
Fig-1.6	Typical Configuration for A Kettle Reboiler [10]	16
Fig-3.1	Geometry Modeling [Design Modular]	22
Fig-3.2	Mesh Generation	23
Fig-4.1	2d Drawing of Kettle Reboiler With 1790mm Dia	32
Fig-4.2	Effect on Pressure (1790mm Dia)	32
Fig-4.3	Effect on Temperature (1790mm Dia)	33
Fig-4.4	Effect on Density (1790mm Dia)	33
Fig-4.5	Effect on Volume Fraction of Phase-2 (1790mm Dia)	33
Fig-4.6	Graph of Mass-Weighted Average of Phase-2 (1790mm Dia)	34
Fig-4.7	2d Drawing of Kettle Reboiler With 1750mm Dia	34
Fig-4.8	Effect on Pressure (1750mm Dia)	35
Fig-4.9	Effect on Temperature (1750mm Dia)	35
Fig-4.10	Effect on Density (1750mm Dia)	35
Fig-4.11	Graph of Mass-Weighted Average of Phase-2 (1750mm Dia)	36
Fig-4.12	2d Drawing of Kettle Reboiler With 1690mm Dia	36
Fig-4.13	Effect on Pressure (1690mm Dia)	37
Fig-4.14	Effect on Density (1690mm Dia)	37
Fig-4.15	Effect on Temperature (1690mm Dia)	37
Fig-4.16	Effect on Vapor Fraction of Phase-2 (1690mm Dia)	38
Fig-4.17	Graph of Mass-Weighted Average of Phase-2 (1690mm Dia)	38

List of Tables

Table No.	Title	Page No.
Table-1.1	Comparison Table of TEMA Heat Exchanger Types (R, C, B)	14
Table-1.2	Nomenclature of Heat Exchanger Components	17
Table-3.1	HTRI Thermal Data Sheet of a Kettle Reboiler	21
Table-3.2	Nozzle Data (Dimension of Nozzle)	21
Table-3.3	Number of Nodes and Elements (1790mm Diameter)	22
Table-3.4	Number of Nodes and Elements (1750mm Diameter)	23
Table-3.5	Number of Nodes and Elements (1690mm Diameter)	23
Table-3.6	System Information (CFD Settings)	23
Table-3.7	Physics Setup	24
Table-3.8	Material Properties	25
Table-3.9	Cell Zone Condition	26
Table-3.10	Boundary Condition	28
Table-3.11	Solver Settings	30
Table-4.1	Comparison of parameters	39
Table-4.2	Cost Comparison	40

Nomenclature

Abbreviation

CFD	Computational Fluid Dynamics
TEMA	Tubular Exchanger Manufacturers Association
HTRI	Heat Transfer Research, Inc.
VOF	Volume of Fluid (Multiphase flow model)
PRESTO	Pressure Staggering Option (Pressure discretization scheme)
HRIC	High-Resolution Interface Capturing (Scheme for VOF)
SIMPLE	Semi-Implicit Method for Pressure-Linked Equations (Solver algorithm)
PISO	Pressure-Implicit with Splitting of Operators (Solver algorithm)
CHF	Critical Heat Flux
ASME	American Society of Mechanical Engineers
DIN	Deutschers Institute für Norming (German standards)
EDR	Exchanger Design and Rating (Aspen EDR® software)
LES	Large Eddy Simulation (Turbulence modeling technique)
ID	Inner Diameter
2D	Two-Dimensional
3D	Three-Dimensional
CPU	Central Processing Unit
OS	Operating System

Symbols and legends

Symbols	**Unit**	**Description**
Cp	kJ/kgK	Specific Heat
ρ	kg/m³	Density
$q^{"}$	W/m²	Heat flux
μ	Pa-sec	Viscosity
k	W/m^2K	Thermal Conductivity

Abstract

Kettle reboilers play a vital role in refinery processes, where the operation has a direct impact on overall system performance. To enhance reliability and minimize operational issues such as liquid carryover, a comprehensive approach involving mechanical optimization and continuous monitoring is essential. This optimization process requires careful evaluation of several critical design and operational parameters, including the entrainment ratio to ensure proper vapor-liquid separation, optimal positioning of inlet and outlet nozzles to maintain flow efficiency, appropriate shell sizing to facilitate effective heat transfer, and assessment of current operating conditions to identify potential improvements. By systematically addressing these factors, refineries can significantly reduce liquid carryover, improve thermal efficiency, and extend the operational lifespan of kettle reboilers, ultimately leading to more stable and cost-effective refinery operations.

ANSYS Fluent software is used for geometric modeling, meshing, thermal simulation, and post-processing. Simulations have been done by varying the shell side diameters of the Kettle Reboiler, with the given boundary conditions as per the problem. The physics of the problem employs a steady-state approach and utilizes a viscous model, specifically the Realizable k-ε turbulence model, and the Eulerian phase change model.

Three simulation trials have been conducted in ANSYS Fluent to analyze the effect of reducing the kettle diameter. The baseline model has a diameter of 1790 mm. And second trial was done with a diameter of 1750 mm, and the third trial was done with a diameter of 1690 mm. The results from the first two trials were approximately the same, both achieving a vapor quality (dryness fraction) of about 0.997. This indicates that a reduction of 40 mm is feasible without compromising performance. This size reduction would save approximately 0.412 feet of sheet metal used in the kettle's fabrication. However, the third trial was conducted on a 1690 mm diameter, resulting in a lower vapor quality of 0.97, which is not acceptable for the application. Therefore, we conclude that the diameter cannot be reduced further than 1750 mm.

Keywords: CFD; Heat Transfer; Kettle Reboiler; Shell and Tube Heat Exchanger; Entrainment Ratio

Chapter 1: Introduction

1.1 Background

Thermal energy control in industrial applications depends significantly on the use of heat exchangers. These systems enable thermal energy exchange across various mediums - including fluids separated by solid walls, fluid-to-surface interactions, or even direct fluid mixing. Their versatility makes them indispensable in diverse sectors, including HVAC systems, power generation, chemical processing, oil refineries, and food production facilities. Among the numerous configurations available, common designs include shell-and-tube, double-pipe, and plate-type exchangers, with our current project focusing on optimizing a shell-and-tube configuration.

The primary function of any heat exchanger is to enable thermal energy exchange between media at different temperatures without external energy input. These systems can handle single substances or complex mixtures, serving multiple purposes such as fluid temperature regulation, phase change processes (evaporation or condensation), and thermal energy recovery. Depending on the application, they may also perform specialized functions like sterilization, distillation, or crystallization. Modern heat exchangers operate on two fundamental principles: recuperative (where fluids remain separated by a heat transfer surface) and regenerative (where thermal energy is alternately stored and released from a matrix). While recuperative designs prevent fluid mixing, regenerative types may experience some cross-contamination between streams due to their operational nature.[1]

1.2 Classification of Heat Exchangers:

Heat exchangers are categorized through multiple classification systems based on their operational and design characteristics. These classification approaches mainly account for elements including:

Heat Transfer Process – Distinguishing between direct-contact and indirect-transfer systems.
Construction Type – Including shell-and-tube, plate, and other structural configurations.
Flow Arrangement – Covering parallel, counterflow, and crossflow designs.
Surface Compactness – Differentiating between compact and non-compact heat transfer surfaces.
Number of Fluids – Two-fluid exchangers are the most common, though multi-fluid systems also exist.
Heat Transfer Mechanism – Classifying based on conduction, convection, or phase-change processes.

Visual representations of these classifications can be found in Figures 1.1 (adapted from Shah [1]) and 1.2 [2], which outline these categories in detail. The following section provides an overview of common heat exchanger types based on construction, along with key selection criteria. For a more comprehensive, see Refs. 1-4.

Various industries frequently utilize tubular heat exchangers because of their flexible operation and sturdy build. These systems can be customized to operate under extreme conditions, ranging from high vacuum environments to ultra-high pressures exceeding 100 MPa (15,000 psig), and from cryogenic temperatures to elevated thermal conditions approaching 1100°C (2000°F). Their versatility extends to handling challenging operational scenarios involving vibration, heavy fouling, corrosive or toxic fluids, and even radioactive materials. Available in various materials including metals, graphite, glass, and Teflon, these exchangers can be designed in sizes ranging from small units (0.1 m^2) to massive installations covering over 100,000 m^2. They find widespread application in petroleum refining, chemical processing, power generation (as condensers,

evaporators, and feedwater heaters), HVAC systems, and waste heat recovery operations. Despite their advantages, shell-and-tube exchangers are inherently non-compact, typically offering 50-100 m^2/m^3 of heat transfer surface area, which results in larger space requirements and higher installation costs compared to compact alternatives. This has led to increasing adoption of compact heat exchangers in applications where operational conditions permit. The design and manufacture of these exchangers follow established standards, including TEMA (Tubular Exchanger Manufacturers Association) classifications, shown in Fig., 1.2,1.3, European DIN norms, and ASME Boiler and Pressure Vessel Codes. The TEMA system uses a three-letter designation (such as BEM or AES) to identify specific front-end, shell, and rear-end configurations, though some specialized designs may not conform to this standardized nomenclature.

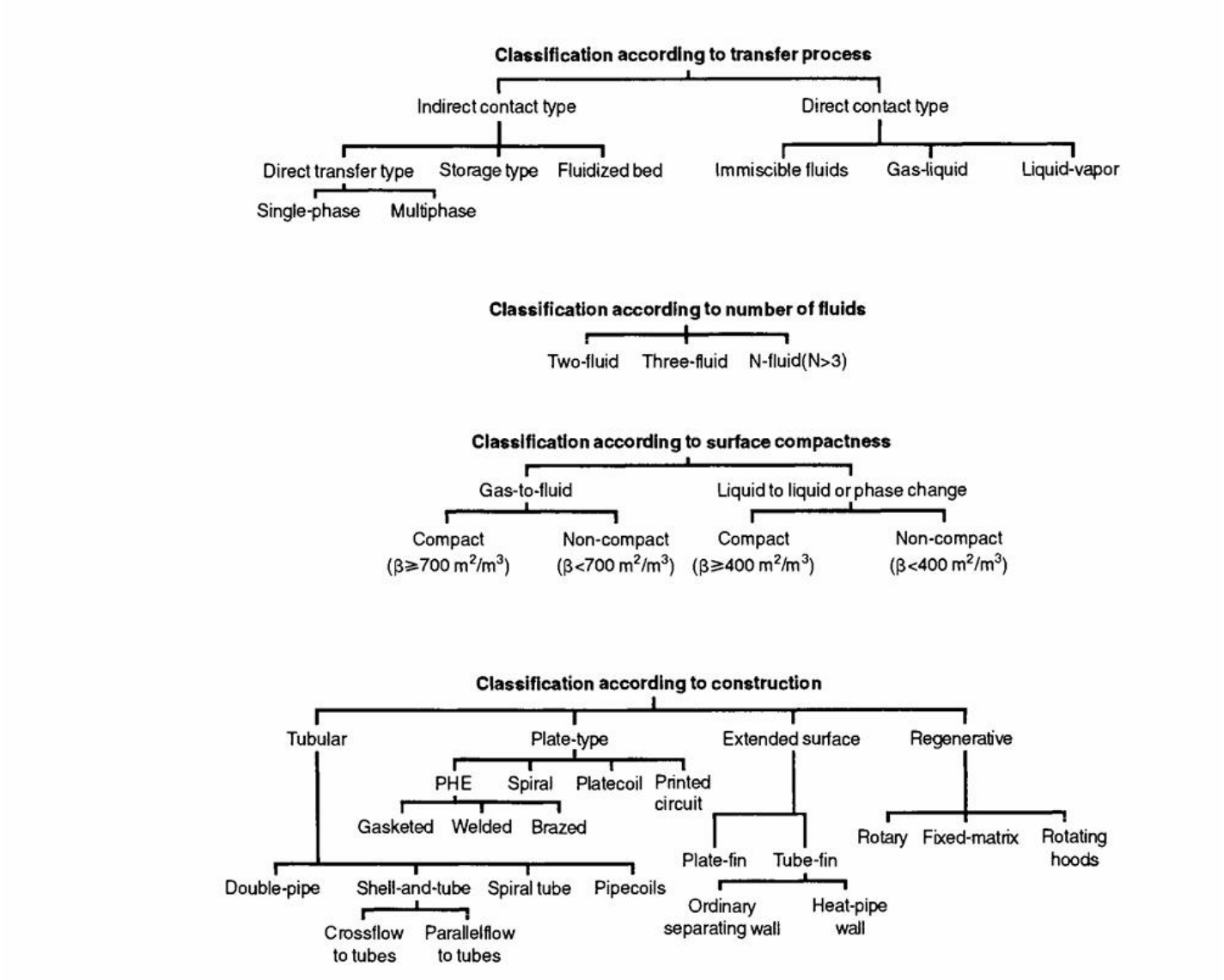

Fig. 1.1: Classification of heat exchangers [1]

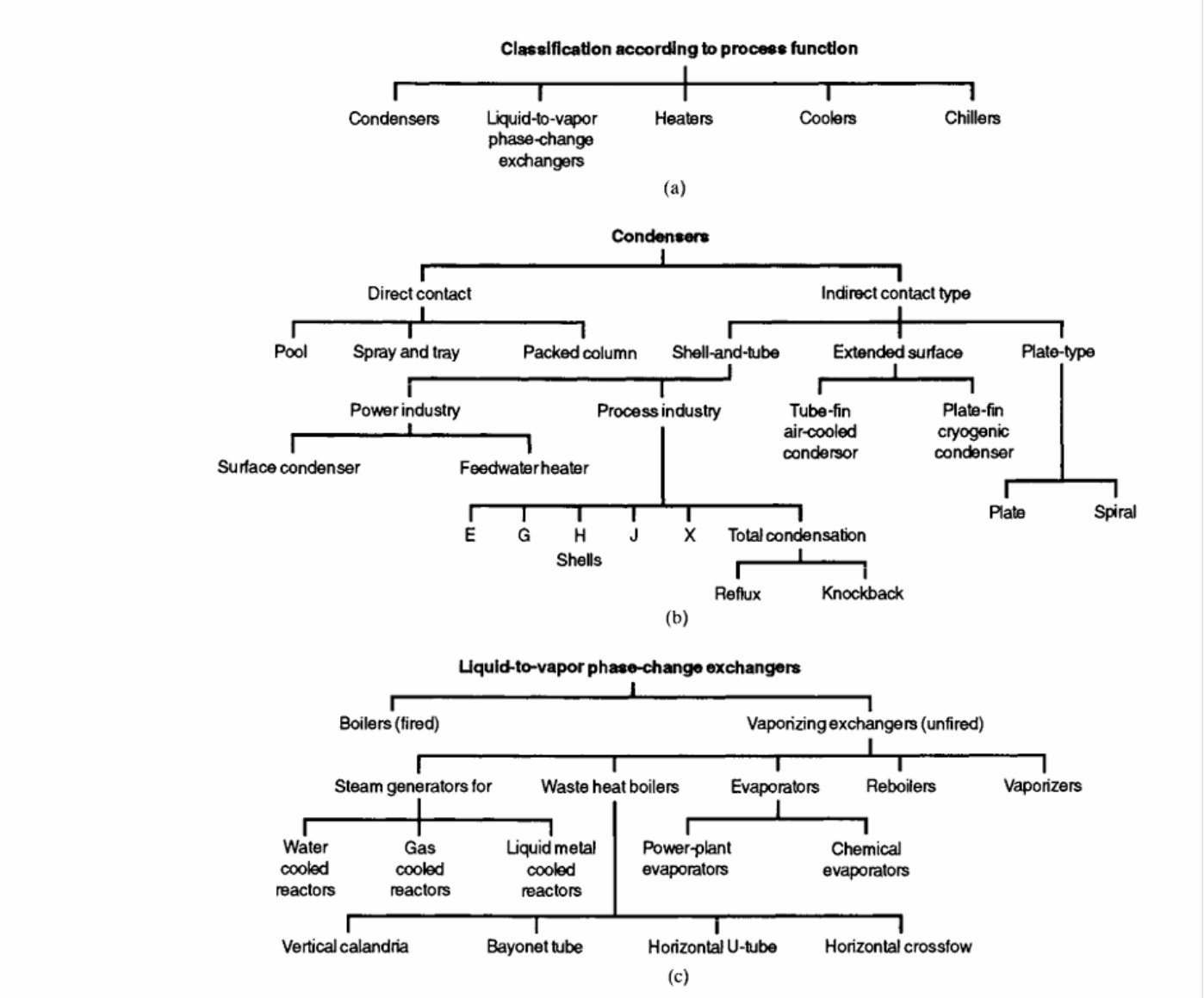

Fig. 1.2: (a) Classification according to process function. (b) Classification of condensers. (c) Classification of liquid-to-vapor phase-change exchangers.[1]

Tubular heat exchangers represent one of the most versatile thermal transfer solutions for industrial applications, offering unmatched flexibility in design and operation. Engineered to withstand some of the most demanding process conditions, these systems reliably function across an extraordinary range of pressures - from complete vacuum states to extreme pressures beyond 15,000 pounds per square inch - while maintaining performance at temperatures spanning from cryogenic levels to nearly 2000°F. Their robust construction allows them to manage difficult operating environments characterized by severe vibration, corrosive media, toxic substances, and significant fouling potential. Manufacturers produce these units using diverse materials ranging from conventional metals to specialized options like corrosion-resistant graphite, transparent glass, and durable Teflon, with heat transfer surfaces scaling from compact 1 ft^2 designs to enormous systems exceeding 1 million square feet. The petroleum and chemical processing industries particularly rely on these exchangers for critical operations, while power plants utilize them extensively for steam condensation, feedwater heating, and oil cooling applications. Their implementation extends to climate control systems and energy recovery projects where maximizing thermal efficiency is paramount. However, the inherent design

characteristics of shell-and-tube configurations result in relatively low surface area density (15-30 ft² per cubic foot), necessitating substantial installation space and supporting infrastructure.

This limitation has driven many industries to adopt more space-efficient compact heat exchangers where process parameters allow. Globally recognized standards, including TEMA specifications, European DIN regulations, and ASME pressure vessel codes, govern their engineering and fabrication. The TEMA classification system employs an alphabetical coding method (examples including BEM and AES configurations) to designate specific mechanical layouts, although certain custom-engineered variants may not fit within this standardized framework.[5]

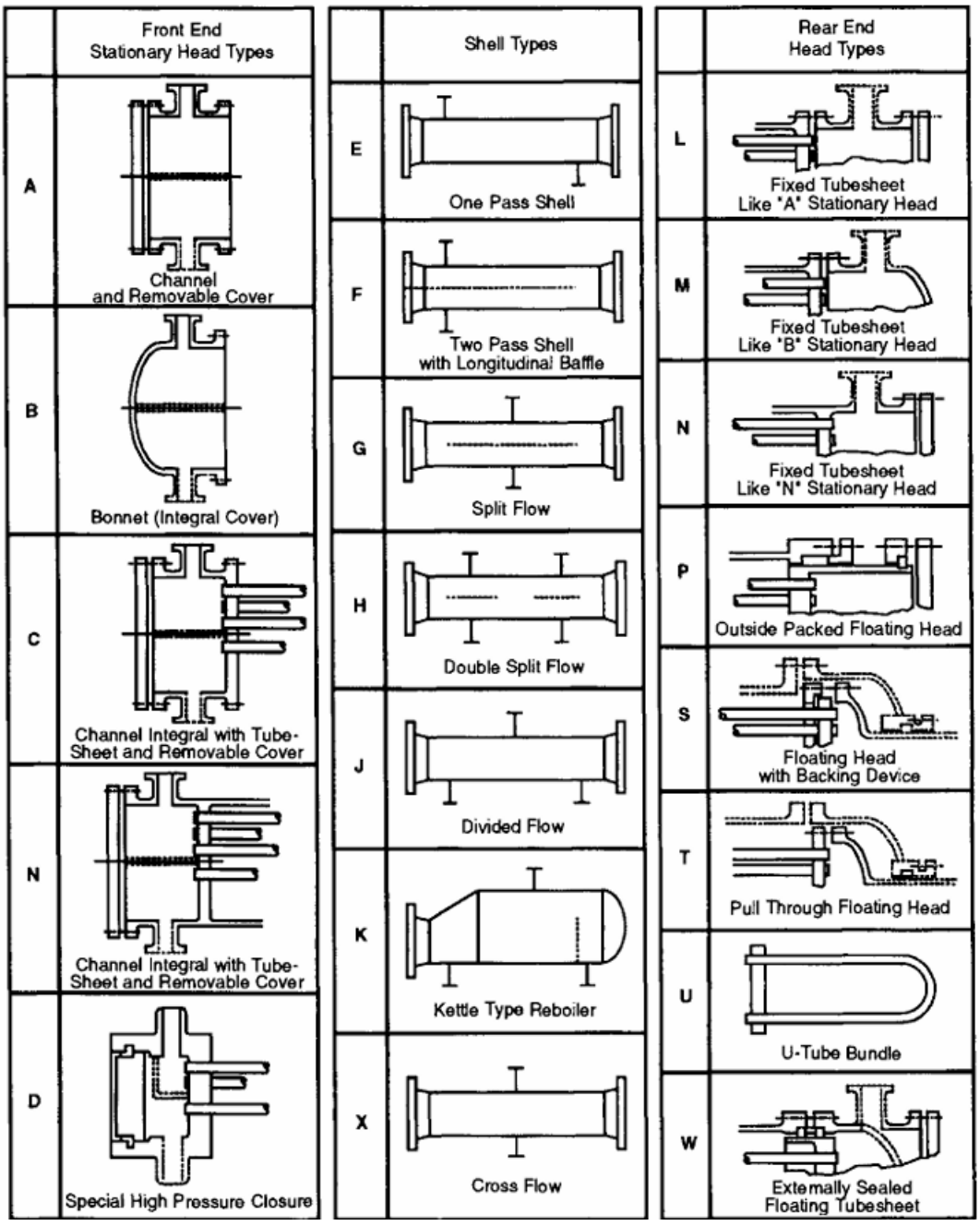

Fig. 1.3: Standard front-end head, shell-type, and rear-end head types, from TEMA [5].

The Tubular Exchanger Manufacturers Association (TEMA) establishes comprehensive guidelines that define critical design parameters for heat exchanger fabrication. These standards precisely outline acceptable manufacturing tolerances across different mechanical classifications, encompassing specifications for tube dimensions (including diameter and pitch configurations), baffle and support plate arrangements, pressure rating categories, and computational methods for determining tube sheet thickness that is required. Engineers must reference these detailed TEMA provisions when designing or evaluating heat exchanger systems to ensure compliance with industry-accepted mechanical and performance standards.

Table 1.1: Design Features of Shell-and-Tube Heat Exchangers [1]

Design features	Fixed tubesheet	Return bend (U-tube)	Outside-packed stuffing box	Outside-packed latern ring	Pull-through bundle	Inside split backing ring
TEMA rear-head type	L, M, N	U	P	W	T	S
Tube bundle removable	No	Yes	Yes	Yes	Yes	Yes
Spare bundles used	No	Yes	Yes	Yes	Yes	Yes
Provides for differential movement between shell and tubes	Yes, with bellows in shell	Yes	Yes	Yes	Yes	Yes
Individual tubes can be replaced	Yes	Yes[a]	Yes	Yes	Yes	Yes
Tubes can be chemically cleaned, both inside and outside	Yes	Yes	Yes	Yes	Yes	Yes
Tubes can be mechanically cleaned on inside	Yes	With special tools	Yes	Yes	Yes	Yes
Tubes can be mechanically cleaned on outside	Yes	Yes[b]	Yes[b]	Yes[b]	Yes[b]	Yes[b]
Internal gaskets and bolting are required	No	No	No	No	Yes	Yes
Double tubesheets are practical	Yes	Yes	Yes	No	No	No
Number of tubesheet passes available	Any	Any even number	Any[c]	One or two[d]	Any[e]	Any[e]
Approximate diametral clearance (mm) (Shell ID–D_{otl})	11–18	11–18	25–50	15–35	95–160	35–50
Relative costs in ascending order, least expensive = 1	2	1	4	3	5	6

[a] Only those in which outside rows can be replaced without special designs.

[b] Outer Area mechanical cleaning possible with square or rotated square pitch, or having a wide triangular pitch.

[c] Axial nozzle is required at the rear end for an odd number of passes.

[d] Tube-side nozzles should be at the stationary end for two passes.

[e] odd number of passes requires a packed gland or bellows at the floating head.

1.3 Schematic Illustration of Shell-And-Tube Heat Exchanger Construction:

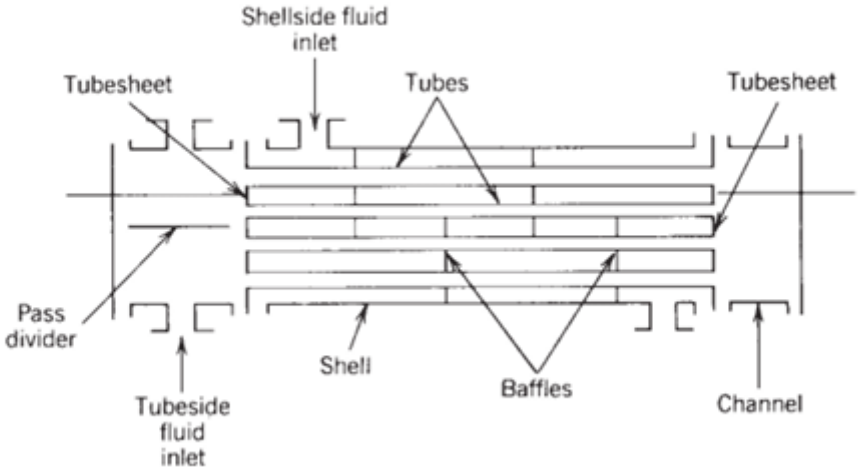

Fig. 1.4: Schematic illustration of shell-and-tube heat exchanger construction [8]

1.4 Kettle Reboilers and Vaporizers:

Kettle reboilers and vaporizers employ a specialized design featuring an enlarged shell section, as described in Figure 1.5. This distinctive configuration serves the critical function of facilitating effective vapor-liquid phase separation. The dimensional parameters of the shell are carefully determined through established engineering correlations that account for the required phase separation efficiency. [9]

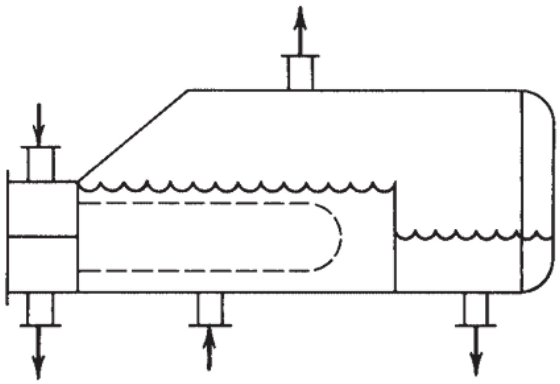

Fig. 1.5: TEMA K-type shell. [5]

To achieve maximum efficiency in kettle reboilers (FIG 1.5), industry standards recommend a shell diameter approximately 1.6-2 times larger than the tube bundle diameter. Critical design considerations must account for three key factors: (1) permissible liquid droplet carryover in the vapor stream, (2) necessary liquid level height above the overflow weir, and (3) adequate freeboard space to accommodate potential foaming conditions. These specifications maintain effective phase segregation and system dependability. [8]

A kettle reboiler, illustrated in (Fig. 1 .6), is a horizontal heat exchanger featuring a TEMA K-type shell that houses either U-tube or straight-tube bundles, which may incorporate finned tubes for enhanced heat transfer. The design utilizes a pull-through floating head (T-type) for ease of maintenance and tube cleaning. Liquid enters through the bottom nozzles via gravity feed from the distillation column's sump, flowing upward across the tube bundle where boiling occurs on the tubes' external surfaces. The oversized shell provides sufficient space above the bundle for effective vapor-liquid separation, with vapor returning to the column while liquid exits over an adjustable weir as bottom product.

This configuration offers several operational advantages, including reliable performance across extreme pressure ranges (from vacuum to near-critical conditions) and effective operation with small temperature differentials through optimized tube spacing. Kettle reboilers outperform thermosyphon designs in extreme pressure environments owing to their natural circulation characteristics and horizontal tube arrangement.

However, the low fluid velocities increase susceptibility to fouling, and the large shell size results in higher capital costs compared to more compact heat exchanger designs. These characteristics make kettle reboilers particularly suitable for services where operational reliability is critical, though proper consideration of fouling potential and initial investment is essential during the design and selection process [10].

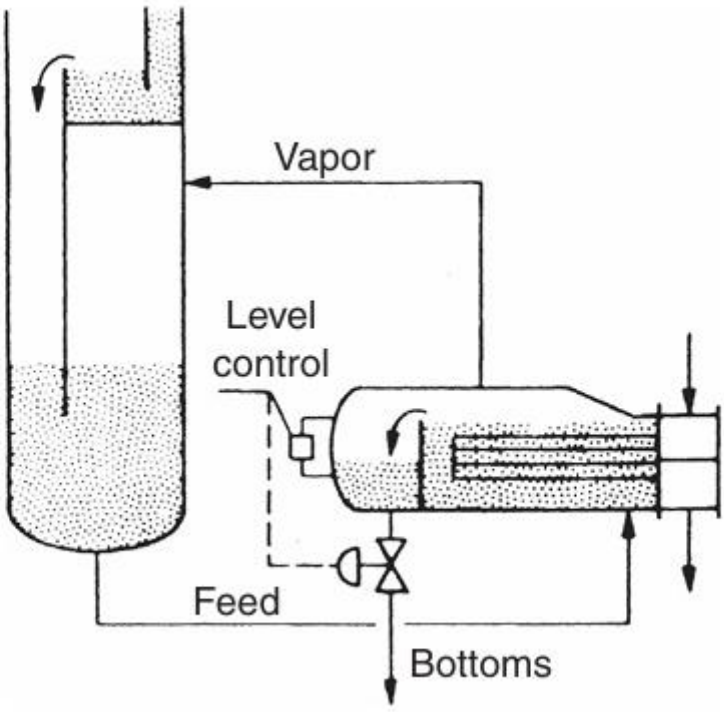

Fig. 1.6: Typical configuration for a kettle reboiler [10]

1.4.1 Reboiler Selection:

The selection of reboiler type is often application-dependent, with certain process conditions favoring specific designs. Severely fouling fluids or highly viscous liquids typically necessitate forced-flow reboilers due to their ability to handle challenging flow conditions. When processing moderately fouling materials with a dirty or corrosive heating medium, horizontal thermosyphon reboilers often emerge as the preferred option. However, many applications present multiple technically viable reboiler configurations, requiring engineers to evaluate alternatives based on key factors including capital and operating costs, operational reliability, process controllability, and demonstrated performance in comparable services. Industry experts like Palen [10] have developed comprehensive selection guidelines (summarized in Table 1.2) that assist in this decision-making process, while Kister [11] provides additional comparative analysis of reboiler types and their optimal application ranges. These resources collectively offer valuable insights for determining the most appropriate reboiler configuration for specific process requirements**.**

Table 1.2: Guidelines For Reboiler Selection

	Reboiler Type			
Process Conditions	Kettle or Internal	Horizontal Shell-Side Thermosyphon	Vertical Tube-Side Thermosyphon	Forced Flow
Operating pressure				
Moderate	E	G	B	E
Near critical	B-E	R	Rd	E
Deep vacuum	B	R	Rd	E
Design ΔT				
Moderate	E	G	B	E
Large	B	R	G-Rd	E
Small (mixture)	F	F	Rd	P
Very small (pure component)	B	F	P	P
Fouling				
Clean	G	G	G	E
Moderate	Rd	G	B	E
Heavy	P	Rd	B	G
Very heavy	P	P	Rd	B
Mixture boiling range				
Pure component	G	G	G	E
Narrow	G	G	B	E
Wide	F	G	B	E
Very wide, with viscous liquid	F-P	G-Rd	P	B

Category abbreviations: B: best; G: good operation; F: fair operation, but a better choice is possible; Rd: risky unless carefully designed, but could be the best choice in some cases; R: risky because of insufficient data; P: poor operation; and E: operable but unnecessarily expensive. Source: Ref. [10]

Chapter 2: Literature Review

2.1 Literature Review:

2.1.1. CFD Modeling of Reboilers

Developed an advanced CFD algorithm for forced recirculating fired reboilers using Fire Dynamics Simulator (FDS) and Large Eddy Simulation (LES) to analyze crude oil boiling. Validated nucleate boiling heat transfer with Chen and Mostinski correlations (error: 10.5%) [12]

Applied a two-fluid CFD model for kettle reboilers, emphasizing interfacial friction effects in two-phase flow across tube bundles. Used porous media approaches for bundle flow resistance [13]

Early CFD work on nuclear evaporators, adapted for reboilers. Highlighted challenges in modeling slip between phases in tube bundles [13]

2.1.2. Thermal-Hydraulic Analysis

Experimental study on kettle reboiler performance, linking void fraction distributions to heat flux (≥10 kW/m²) and recirculation rates [12] [14]

Measured boiling regimes in tube bundles, showing rapid void fraction increases with heat flux. Noted limitations of 1D models for lateral flow prediction [12] [14]

Derived empirical correlations for void fraction and slip in two-phase flow, critical for shell-side thermal-hydraulics [12]

2.1.3. Diameter Optimization & Geometric Effects

Used Aspen EDR® to optimize kettle reboiler diameter (25.4 mm) and material (cast iron), improving efficiency by 28.27% [15] [28]

Studied foam formation in reboiler bundles, noting disengagement challenges at high heat fluxes (30 kW/m²) and implications for diameter selection [12]

Investigated pitch-to-diameter ratios in tube bundles, showing staggered arrangements enhance heat transfer [12]

2.1.4. Two-Phase Flow & Boiling Mechanisms

Seminal work on nucleate boiling correlations (e.g., Forster-Zuber, Dittus-Boelter), widely used in reboiler CFD studies [12]

Experimental data on hydrocarbon boiling regimes, foundational for critical heat flux (CHF) predictions in reboilers [14]

Developed two-fluid models for interfacial drag in boiling flows, later adapted for reboiler CFD [12] [32]

2.1.5. Advanced Numerical Approaches

Applied PHOENICS CFD with two-fluid models, revealing sensitivity to interfacial drag coefficients in void fraction predictions [14]

Early CFD work on two-phase flow, influencing later reboiler simulations [14]

Integrated CFD with field data for boilers, validating heat transfer parameters (emissivity, fouling) relevant to reboiler design [16] [19]

2.2 Research Gap:

Research Gaps in Kettle Reboiler Diameter Optimization

Lack of CFD Studies on Diameter-Dependent Flow Maldistribution

Most CFD studies (Rahman et al., 1996) focus on tube bundles but neglect how kettle diameter affects shell-side flow uniformity, especially in large-diameter designs.

Limited Data on Vapor Disengagement Efficiency vs. Diameter

While King & Jensen (1995) studied foam formation, no systematic CFD/experimental work correlates kettle diameter with vapor escape velocity to prevent liquid entrainment.

Insufficient Models for Vapor Quality Prediction at Different Diameters

Empirical correlations (Chen, 1966) predict heat transfer but lack diameter-specific vapor quality models, critical for distillation column feed.

Over-Reliance on 2D Simulations for 3D Phase Separation

Many studies (Edwards & Jensen, 1991) use simplified 2D models, ignoring 3D vortex formation in large-diameter kettles that disrupt phase separation.

Neglect of High-Viscosity Fluid Behavior in Diameter Optimization

Existing work (Alsaemre et al., 2022) optimizes diameter for water/light hydrocarbons but not for high-viscosity fluids, where flow regimes differ.

No Universal Criteria for Optimal Diameter-to-Length Ratio

While Dowlati et al. (1992) optimized tube pitch, no guidelines exist for kettle aspect ratio (D/L) balancing heat transfer vs. vapor disengagement.

Inadequate Validation of CFD with Real-Scale Kettle Data

Most validations (Davidy, 2020) use lab-scale setups; industrial-scale experimental data for diameter effects are scarce.

Gap in Coupling Thermal Performance with Mechanical Constraints

Studies rarely address how diameter changes impact structural stress (e.g., ASME code compliance) alongside thermal efficiency.

2.3 Research Objectives:

1. To analyze the effect of kettle diameter on fluid flow distribution and heat transfer.
2. To optimize the shell-side vapor disengagement area for efficient phase separation.
3. To determine the quality of the vapor at the outlet for a given kettle diameter.
4. To minimize the cost of the kettle reboiler

Chapter 3: Methodology

3.1 Problem Statement

The design and operation of kettle reboilers must ensure optimal entrainment ratio, nozzle, shell sizing, and vapor-liquid separation efficiency to maintain performance while minimizing costs. In this study, the current reboiler diameter (1790 mm) is compared after reducing the reboiler diameter (1750 mm) to evaluate whether downsizing affects vapor quality (dryness fraction ~0.997) and liquid carryover. Despite the reduction, simulations in ANSYS Fluent show nearly identical performance, suggesting potential material savings (0.412 feet of sheet metal per reboiler). However, further validation is needed to confirm that the smaller diameter does not compromise fluid dynamics, heat transfer, or long-term operational stability.

There is no direct formula to derive the kettle reboiler diameter. In the HTRI manual, there is an iterative procedure to derive the kettle diameter on the basis of tube bundle diameter and engineering experience.

In Table 3.1, take an HTRI sheet to perform the simulation, and the data of the kettle reboiler.

Table 3.1: HTRI Thermal data sheet of a kettle reboiler

	HTRI	**HEAT EXCHANGER RATING DATA SHEET**				
		Released to the following HTRI Member Company:				**Air Products Units**
		ISGEC				
		NITISH				
	Service of Unit MP Steam Generator			Item No. 201-E313		
	Type CKU	Orientation Horizontal		Connected In 1 Parallel	1 Series	
	Surf/Unit (Gross/Eff) 210.57 / 190.82 m2	Shell/Unit 1		Surf/Shell (Gross/Eff) 210.57 / 190.82 m2		
	PERFORMANCE OF ONE UNIT					
	Fluid Allocation		Shell Side		Tube Side	
	Fluid Name		Water/Steam		Syngas	
	Fluid Quantity, Total	kg/hr	11114		463201	
	Vapor (In/Out)	wt%	0.00	97.00	100.00	100.00
	Liquid	wt%	100.00	3.00	0.00	0.00
	Temperature (In/Out)	C	110.60	257.02	317.50	294.20
	Density	kg/m3	952.58	22.534 V/L 788.26	19.652	20.450
	Viscosity	mN-s/m2	0.2544	0.0178 V/L 0.1030	0.0248	0.0239
	Specific Heat	kJ/kg-C	4.2209	4.2150 V/L 4.9441	2.3953	2.3991
	Thermal Conductivity	W/m-C	0.6839	0.0533 V/L 0.6093	0.1205	0.1160
	Critical Pressure	bar				
	Inlet Pressure	bar	44.800		62.800	
	Velocity	m/s		0.14		37.70
	Pressure Drop, Allow/Calc	bar		0.125		0.887
	Average Film Coefficient	W/m2-K	9514.4		3928.4	
	Fouling Resistance (min)	m2-K/W	0.000176		0.00022	
	Heat Exchanged	7.0440 MegaWatts	MTD (Corrected)	49.2 C	Overdesign	38.75 %
	Transfer Rate, Service	750.53 W/m2-K	Calculated	1041.3 W/m2-K	Clean	1953 W/m2-K

Table 3.2: Nozzle Data

Shell Inlet Dia	76.200 mm
Shell Outlet Dia	101.60 mm
Inlet Nozzle Height	89.375 mm
Outlet Nozzle Height	104.38mm

Table 3.3: System Information

Application	Fluent
Settings	3d, double precision, pressure-based, Eulerian, realizable k-epsilon
Version	22.1.0-10213
Source Revision	91b44bc38e
CPU	11th Gen Intel(R) Core (TM) i7-1115G4 @ 5.00GHz
OS	Windows

3.2 Numerical Simulation:

3.2.1 Geometry modeling:

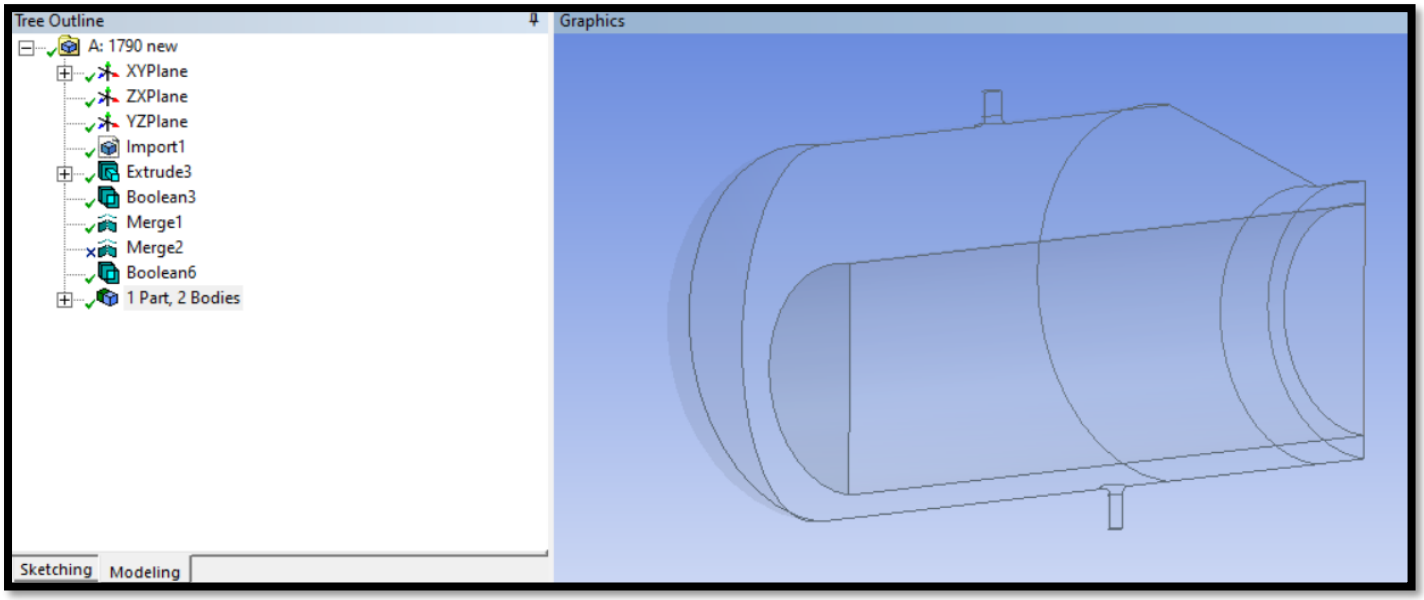

Fig. 3.1: Geometry Modeling [Design modular]

In **Design Modular**, the **Extrude**, **Boolean**, and **Merge** commands that as shown in (Fig. 3 .1), are powerful tools for transforming and manipulating 3D geometry in architectural and modular design. The **Extrude** command is used to give depth to 2D shapes, such as turning a floor plan into walls or a flat sketch into a 3D object by pulling it along an axis. The **Boolean** operations—**Union**, **Subtract**, and **Intersect**—allow designers to combine, cut, or retain overlapping sections of 3D objects, enabling the creation of complex structures like custom-built cabinetry or openings in walls. Meanwhile, the **Merge** command simplifies models by seamlessly joining separate objects into a single mesh, which is useful for refining modular components or preparing designs for fabrication. Together, these commands streamline workflows, enhance precision, and enable the creation of intricate, customizable designs in **Design Modular.**

3.2.2 Mesh modeling:

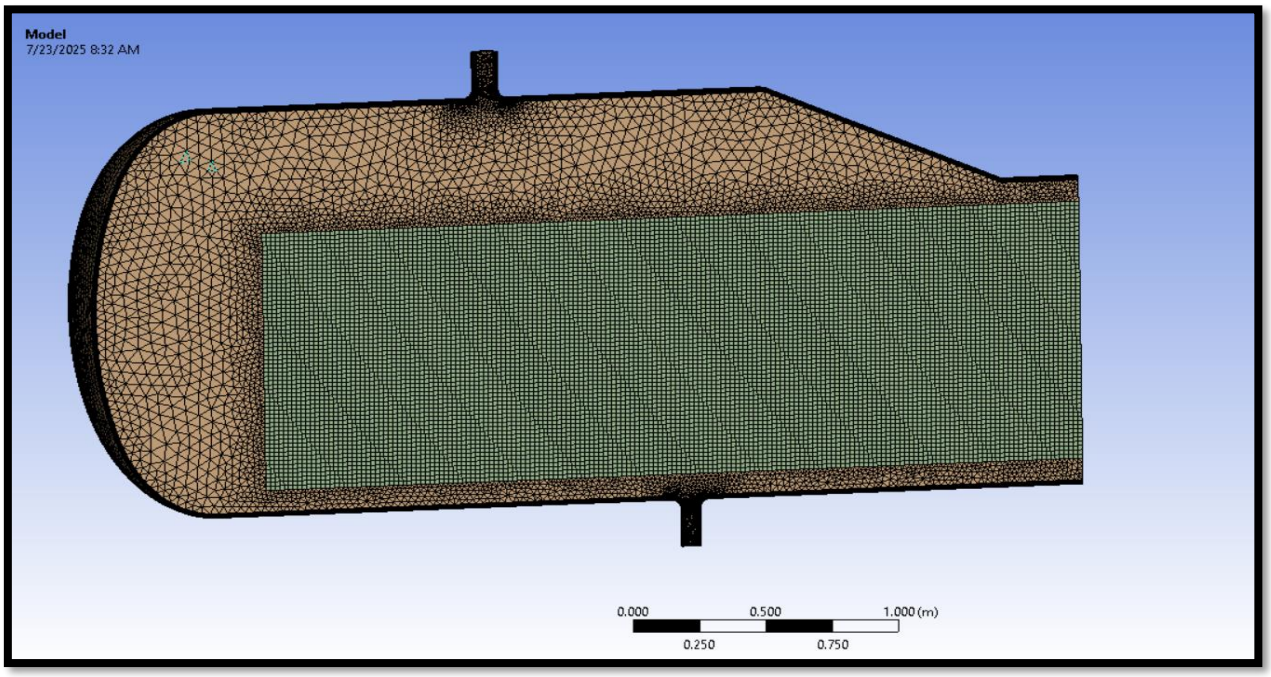

Fig 3.2: Mesh Generation

Table 3.4: No of Elements with Kettle Diameter 1790mm

Domain	Nodes	Elements
Part_2 Domain	289727	1070554
Part_2 hs	314640	298930
All Domains	604367	1369484

Table 3.5: No of Elements with Kettle Diameter 1750mm

Domain	Nodes	Elements
Part_2 Domain	288576	1065232
Part_2 hs	316440	300541
All Domains	605016	1365773

Table 3.6: No of Elements with Kettle Diameter 1690 mm

Domain	Nodes	Elements
Part_2 Domain	288576	1065232
Part_2 hs	316440	300541
All Domains	605016	1365773

3.3 Physics:

3.3.1 Model:

Table 3.7: Physics Setup

Model	Settings
Space	3D
Time	Steady
Viscous	Realizable k-epsilon turbulence model
Wall Treatment	Scalable Wall Function
Multiphase k-epsilon Models	Mixture k-epsilon
Heat Transfer	Enabled
Multiphase	Eulerian

Viscous Model "Realizable k-epsilon turbulence model":

The Realizable k-ε turbulence model is an improved version of the standard k-ε model, designed to provide more accurate predictions for complex flows, including those with strong streamline curvature, vortices, and separation. Unlike the standard k-ε model, the Realizable variant introduces a variable turbulent viscosity formulation and a modified transport equation for the dissipation rate (ε) to ensure physically realistic results, particularly in regions of high strain rates and rotating flows. [37]

1. Turbulent Kinetic Energy (k) Equation:

$$\frac{\partial(\rho k)}{\partial t} + \frac{\partial(\rho k u_j)}{\partial x_j} = \frac{\partial}{\partial x_j}\left[\left(\mu + \frac{\mu_t}{\sigma_k}\right)\frac{\partial k}{\partial x_j}\right] + G_k + G_b - \rho\epsilon - Y_M \tag{3.1}$$

where:

G_k = Turbulence production due to mean velocity gradients
G_b = Buoyancy turbulence production
Y_M = Contribution from compressibility effects
μ_t = Turbulent viscosity $(\mu_t = \rho C_\mu \frac{k^2}{\epsilon})$

2. Dissipation Rate (ε) Equation (Modified for Realizability):

$$\frac{\partial(\rho\epsilon)}{\partial t} + \frac{\partial(\rho\epsilon u_j)}{\partial x_j} = \frac{\partial}{\partial x_j}\left[\left(\mu + \frac{\mu_t}{\sigma_\epsilon}\right)\frac{\partial \epsilon}{\partial x_j}\right] + \rho C_1 S\epsilon - \rho C_2 \frac{\epsilon^2}{k + \sqrt{\nu\epsilon}} + C_{1\epsilon}\frac{\epsilon}{k}C_{3\epsilon}G_b \tag{3.2}$$

Where:

$$C_1 = \max\left[0.43, \frac{\eta}{\eta+5}\right]$$
$$\eta = S\frac{k}{\epsilon}$$
$$S = \sqrt{2S_{ij}S_{ij}} \text{ (mean strain rate tensor)}$$

The Eulerian multiphase model in ANSYS Fluent is a powerful computational method for simulating interacting phases (gas-liquid, liquid-solid, etc.) where each phase is treated as a continuous medium with its flow field. This approach is particularly useful for analyzing kettle reboilers, bubble columns, fluidized beds, and other multiphase systems. Accurate Phase Interaction Modeling. Each phase has its velocity, temperature, and volume fraction equations. Captures momentum exchange (drag, lift, virtual mass forces) and heat/mass transfer between phases. Essential for predicting boiling, condensation, and vapor-liquid separation in reboilers.

3.3.2 Material Properties: **Table 3.8:** Material Properties

▬ Fluid	
▬ water-liquid	
Density	polynomial
Cp (Specific Heat)	polynomial
Thermal Conductivity	polynomial
Viscosity	polynomial
Molecular Weight	18.0152 kg/kmol
Standard State Enthalpy	0
Reference Temperature	298.15 K
Thermal Expansion Coefficient	0
Speed of Sound	none
▬ water-vapor	
Density	23.75 kg/m^3
Cp (Specific Heat)	4221 J/(kg K)
Thermal Conductivity	0.0528 W/(m K)
Viscosity	1.79e-05 kg/(m s)
Molecular Weight	18.01534 kg/kmol
Standard State Enthalpy	29923000 J/kgmol
Reference Temperature	298.15 K
Thermal Expansion Coefficient	0
Speed of Sound	none
▬ air	
Density	1.225 kg/m^3
Cp (Specific Heat)	1006.43 J/(kg K)
Thermal Conductivity	0.0242 W/(m K)
Viscosity	1.7894e-05 kg/(m s)
Molecular Weight	28.966 kg/kmol
Standard State Enthalpy	0
Reference Temperature	298.15 K
Thermal Expansion Coefficient	0
Speed of Sound	none
▬ Solid	
▬ steel	
Density	8030 kg/m^3
Cp (Specific Heat)	502.48 J/(kg K)
Thermal Conductivity	16.27 W/(m K)
▬ aluminum	
Density	2719 kg/m^3
Cp (Specific Heat)	871 J/(kg K)
Thermal Conductivity	202.4 W/(m K)

3.3.3 Cell Zone Conditions:

Table 3.9: Cell Zone Condition

━ Fluid	
━ part_2-hs (mixture)	
Specify source terms?	no
Specify fixed values?	no
Frame Motion?	no
Laminar zone?	no
Porous zone?	yes
Porosity	0.4975
Enable Relative Permeability?	yes
Maximum Capillary Pressure [Pa]	1e+07
Equilibrium Thermal Model (if no, Non-Equilibrium)?	yes
Solid Material Name	steel
3D Fan Zone?	no
━ part_2-hs (phase-1)	
Conical porous zone?	no
X-Component of Direction-1 Vector	1
Y-Component of Direction-1 Vector	0
Z-Component of Direction-1 Vector	0
X-Component of Direction-2 Vector	0
Y-Component of Direction-2 Vector	1
Z-Component of Direction-2 Vector	0
Relative Velocity Resistance Formulation?	yes
Direction-1 Viscous Resistance [m^-2]	0
Direction-2 Viscous Resistance [m^-2]	46.6
Direction-3 Viscous Resistance [m^-2]	46.6
Choose an alternative formulation for inertial resistance?	no
Direction-1 Inertial Resistance [m^-1]	0
Direction-2 Inertial Resistance [m^-1]	452
Direction-3 Inertial Resistance [m^-1]	452
C0 Coefficient for Power-Law	0
C1 Coefficient for Power-Law	0
Relative Viscosity	1
━ part_2-hs (phase-2)	
Conical porous zone?	no
X-Component of Direction-1 Vector	1
Y-Component of Direction-1 Vector	0
Z-Component of Direction-1 Vector	0
X-Component of Direction-2 Vector	0

3.3.4 Boundary Conditions:

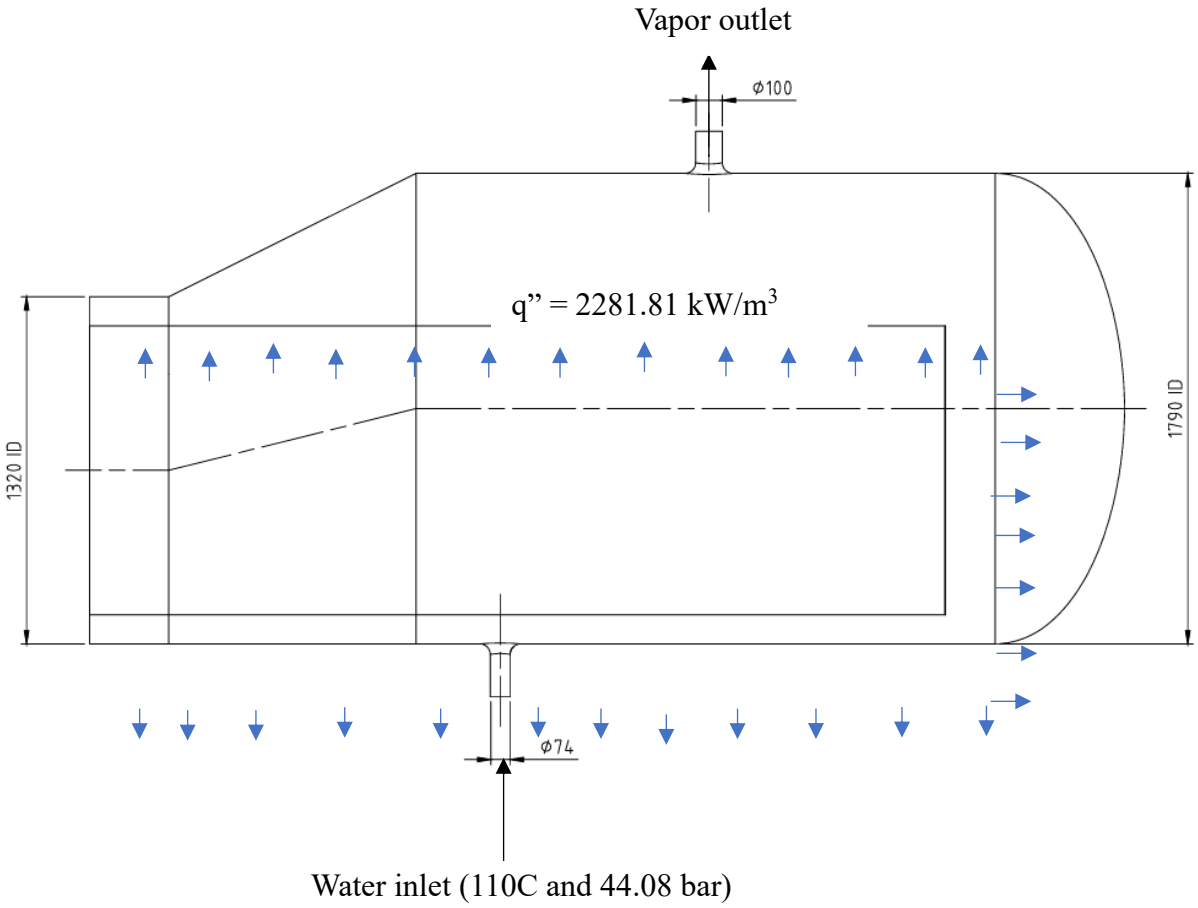

Fig. 3.2: Boundary Condition

Heat generation rate:

Total heat generation (Q) = 7.044 MW = 7.044 × 10^6 W

Diameter of the cylinder (D) = 1.1 m → Radius (r) = 1.12=0.55 m21.1=0.55m

Length of the cylinder (L) = 3.25 m

Calculate the Volume of the Cylinder

The volume V_V of a cylinder is given by:

$V=\pi r^2 L$

$V=\pi$ (0.55)2(3.25)

≈3.088 m^3

Compute the Heat Generation Rate per Unit Volume

$q'' = \frac{Q}{v} = \frac{7.044 \times 10^6}{3.088}$ =2281817.78W/m^3

Momentum Equations (Navier–Stokes Equations)

These equations describe the motion of the fluid under the influence of pressure, viscous forces, and body forces

$$\rho\,(\partial V/\partial t + V \cdot \nabla V) = -\nabla P + \mu \nabla^2 V + F \qquad (3.3)$$

Where:
ρ = fluid density
μ = dynamic viscosity
P = pressure
F = body forces (e.g., gravity)
V= fluid velocity
t = time

Energy Equation (Heat Transfer Equation)

Used to model heat transfer, including boiling and condensation phenomena:

$$\rho C_p\,(\partial T/\partial t + V \cdot \nabla T) = \nabla \cdot (k\,\nabla T) + Q \qquad (3.4)$$

Where:
Cp = specific heat capacity
T = temperature
k = thermal conductivity
Q = heat source term (e.g., from heated walls)

Table 3.10: Boundary Condition

━ Inlet	
━ inlet (mixture)	
Reference Frame	Absolute
Supersonic/Initial Gauge Pressure [Pa]	0
Direction Specification Method	Direction Vector
Coordinate System	Cartesian (X, Y, Z)
Turbulent Specification Method	Intensity and Hydraulic Diameter
Turbulent Intensity [%]	1
Hydraulic Diameter [m]	0.2
━ inlet (phase-1)	
Mass Flow Specification Method	Mass Flow Rate
Mass Flow Rate [kg/s]	1.54361
Total Temperature [K]	383.15
Component of Flow Direction (x, y,z)	(0, 1, 0)
━ inlet (phase-2)	
Mass Flow Specification Method	Mass Flow Rate
Mass Flow Rate [kg/s]	0
Total Temperature [K]	530.55
Component of Flow Direction (x,y,z)	(0, 1, 0)
Slip Velocity Specification Method	Velocity Ratio
Phase Velocity Ratio	1

▬ Outlet	
▬ outlet (mixture)	
Gauge Pressure [Pa]	0
Pressure Profile Multiplier	1
Backflow Direction Specification Method	Normal to Boundary
Turbulent Specification Method	Intensity and Hydraulic Diameter
Backflow Turbulent Intensity [%]	1
Backflow Hydraulic Diameter [m]	0.2
Radial Equilibrium Pressure Distribution	no
▬ outlet (phase-1)	
Backflow Total Temperature [K]	530.55
▬ outlet (phase-2)	
Backflow Total Temperature [K]	530.55
Volume Fraction Specification Method	Backflow Volume Fraction
Backflow Volume Fraction	1
▬ Symmetry	
symmetry-part_2-hs (mixture)	
symmetry-part_2-hs (phase-1)	
symmetry-part_2-hs (phase-2)	
symmetry-part_2-domain (mixture)	
symmetry-part_2-domain (phase-1)	
symmetry-part_2-domain (phase-2)	
▬ Wall	
▬ wall-part_2-domain (mixture)	
Wall Thickness [m]	0
Heat Generation Rate [W/m^3]	0
Material Name	steel
Thermal BC Type	Heat Flux
Heat Flux [W/m^2]	0
Enable shell conduction?	no
Wall Motion	Stationary Wall
Wall Roughness Height [m]	0
Wall Roughness Constant	0
Convective Augmentation Factor	1
wall-part_2-domain (phase-1)	
wall-part_2-domain (phase-2)	
▬ side_face-part_2-hs (mixture)	
Wall Thickness [m]	0
Heat Generation Rate [W/m^3]	0
Material Name	steel
Thermal BC Type	Heat Flux
Heat Flux [W/m^2]	0
Enable shell conduction?	no
Wall Motion	Stationary Wall

3.3.5 Solver Settings:

The Coupled solution method in ANSYS Fluent is a pressure-based solver algorithm that solves the momentum and pressure-based continuity equations simultaneously (strongly coupled) instead of sequentially (like the SIMPLE or PISO methods). This approach is particularly useful for complex, high-speed, or multiphase flows.
Improved Performance for Multiphase Flows (Eulerian Model)
Since this study involves vapor-liquid separation (Eulerian multiphase), the Coupled solver helps maintain phase interaction stability.
Reduces oscillations in volume fraction calculations

Table 3.11: Solver Settings

− Equations	
Flow	True
Volume Fraction	True
Turbulence	True
Energy	True
− Numerics	
Absolute Velocity Formulation	True
− Pseudo Time Explicit Relaxation Factors	
Density	1
Body Forces	0.5
Vaporization Mass	0.5
Volume Fraction	0.3
Turbulent Kinetic Energy	0.3
Turbulent Dissipation Rate	0.3
Turbulent Viscosity	0.5
Energy	0.6
Explicit Momentum	0.3
Explicit Pressure	0.3
− Pressure-Velocity Coupling	
Type	Coupled
Pseudo Time Method (Global Time Step)	True
− Discretization Scheme	
Pressure	PRESTO!
Momentum	Second Order Upwind
Volume Fraction	Modified HRIC
Turbulent Kinetic Energy	First Order Upwind
Turbulent Dissipation Rate	First Order Upwind
Energy	Second Order Upwind

Chapter 4: Results and Discussion

We conducted a study with three test cases to evaluate the effect of kettle diameter on vapor quality. The diameters analyzed were 1790 mm (the baseline from the operational data), 1750 mm, and 1690 mm. The objective was to determine if and how this geometric change impacts the quality of the generated vapors. The following section compares and analyzes the results from these simulations.4.1 Case 1 (Kettle Diameter 1790mm):

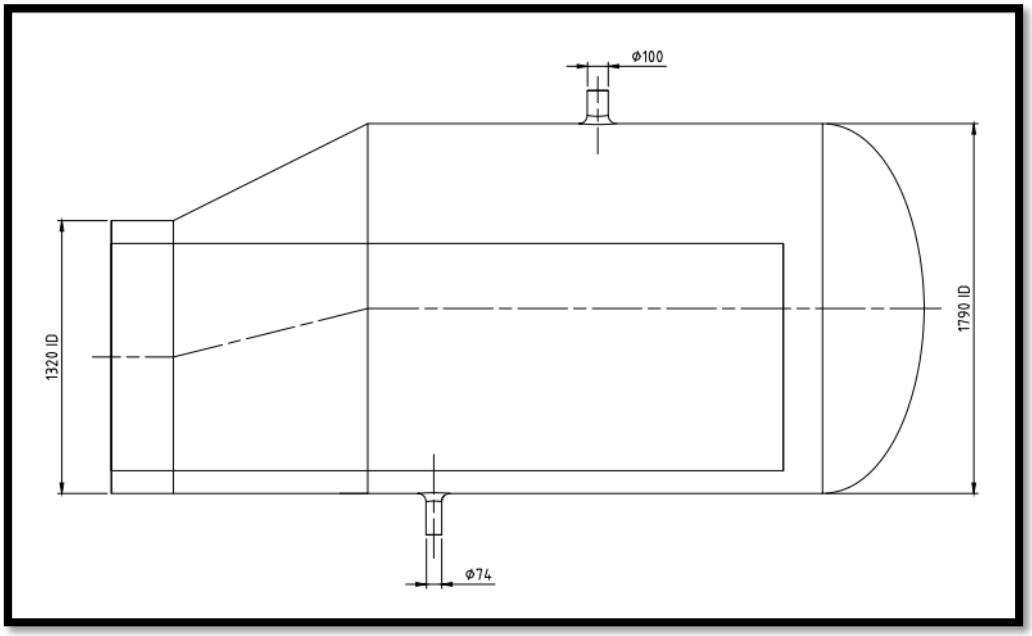

Fig. 4.1: 2d Drawing of Kettle Reboiler with 1790mm Diameter

4.1.1 Effect on Pressure:

The color legend in Fig. 4.2 indicates absolute pressure from 4,478,673 Pa (~44.79 bar) to 4,493,262 Pa (~44.93 bar).

This is a very small pressure drop (only ~14.5 kPa) across the entire domain,

Pressure gradient is vertical indicating natural convection or phase change behavior (liquid-vapor interface or stratification)

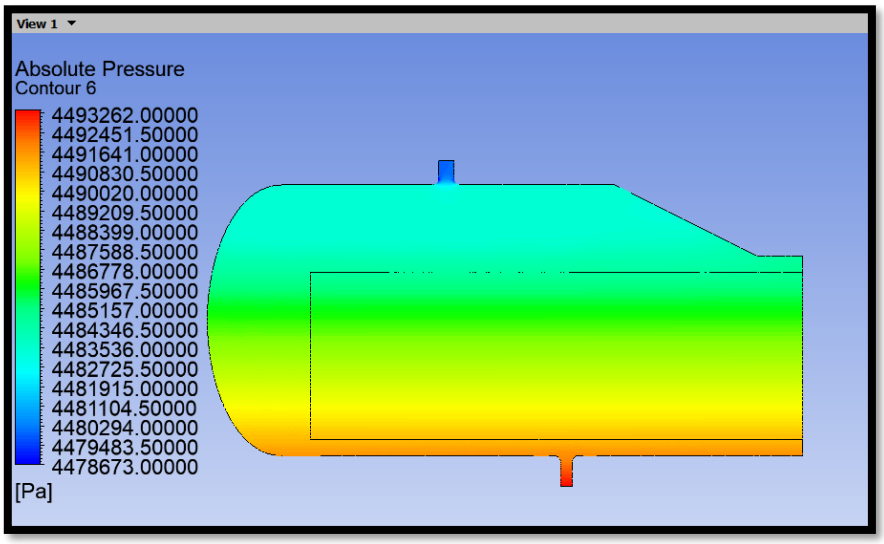

Fig. 4.2: Effect on Pressure

4.1.2 Effect on Temperature:

Subcooled liquid enters at ~383 K and is heated via the reboilers tube bundle.

Boiling occurs in the yellow-orange zone, with vapor rising to the top.

Superheated vapor forms and accumulates in the top chamber (red region). That is shown in Fig. 4.3

The system is functioning as expected: heating → boiling → superheating → vapor exit.

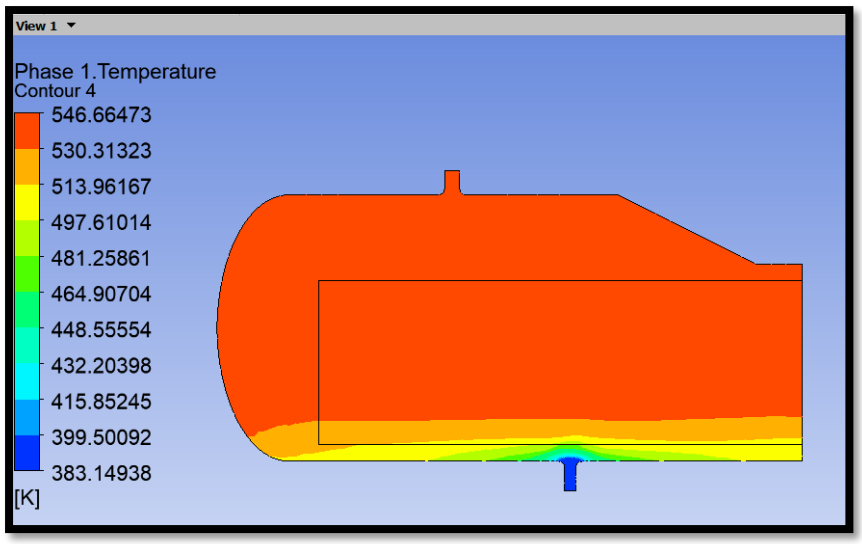

Fig. 4.3: Effect on Temperature

4.1.3 Effect on Density:

Bottom Region (green–yellow–red): High density → liquid phase

Top Region (blue–cyan): Low density → vapor phase in (Fig. 4.4)

A clear interface (transition zone from green to blue) marks the liquid-vapor boundary, which is typical in boiling simulations.

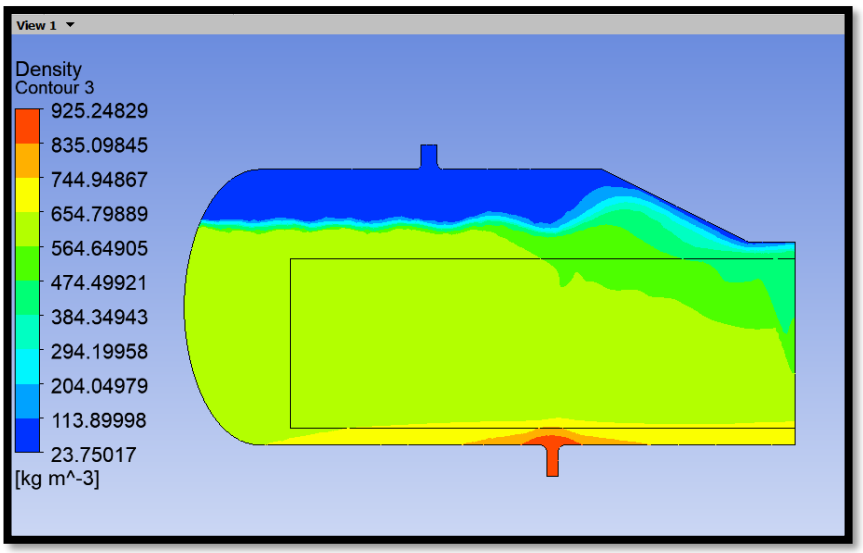

Fig. 4.4: Effect on Density

4.1.4 Effect on Volume Fraction of Phase-2 (water vapor):

Phase 2 Volume Fraction varies from 0.0 (blue) to 1.0 (red):

0.0: 100% liquid phase (no vapor)

1.0: 100% vapor phase (no liquid)

Intermediate (Fig.4.5) colors (green/yellow/orange): mixture regions (boiling interface or foam-like zones)

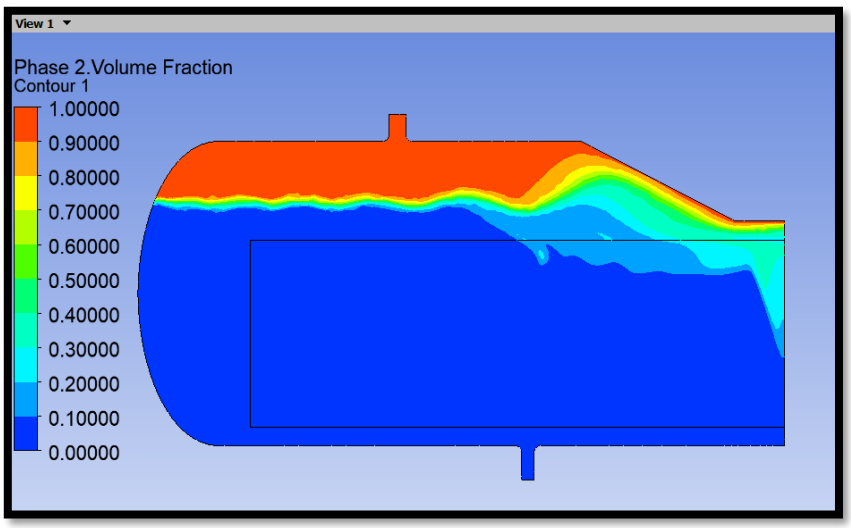

Fig. 4.5: Effect on Volume Fraction of Phase-2(vapor)

4.1.5 Graph of mass-weighted Average of phase-2:

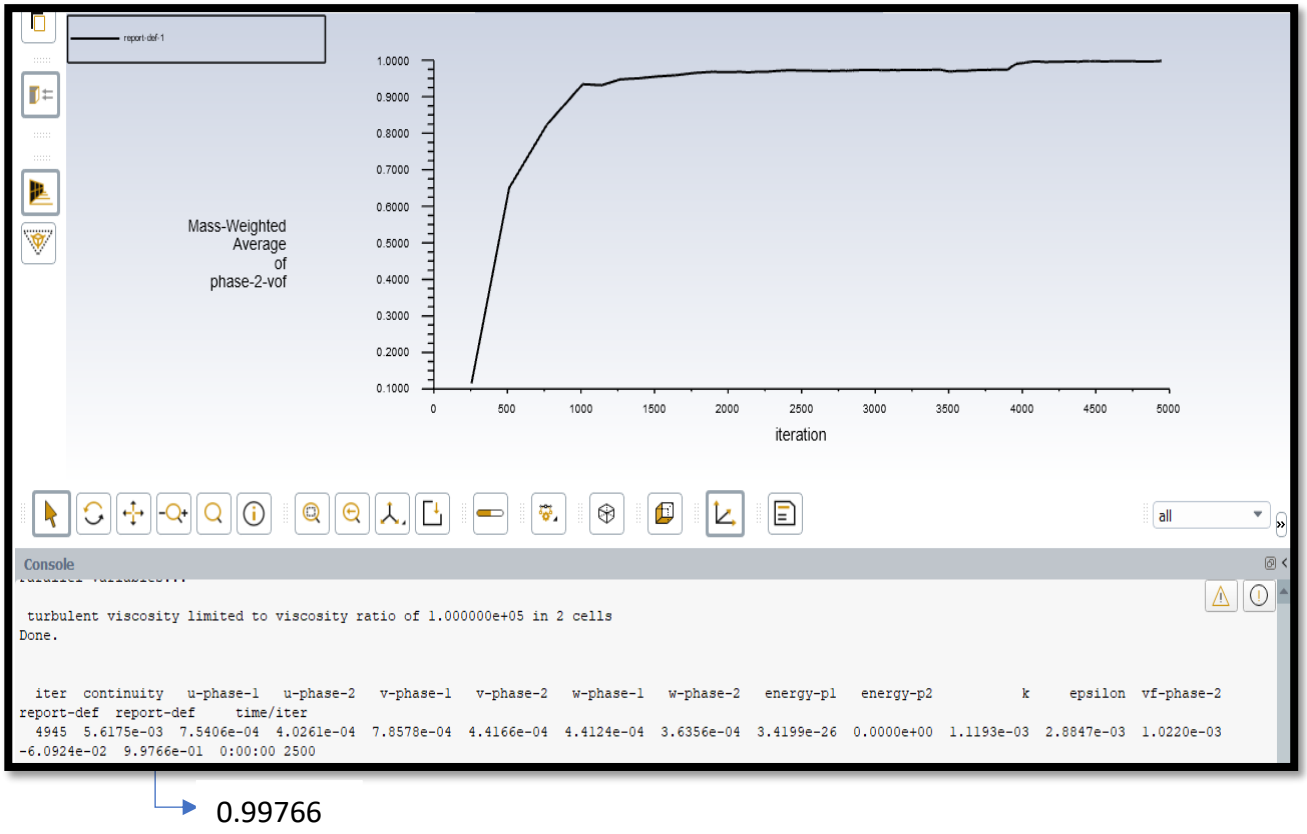

Fig. 4.6: Graph of mass-weighted Average of phase 2(vapor)

The simulation has likely converged, as indicated in Figure 4.6, or is very close to convergence. The vapor fraction has stabilized at approximately 0.99766, indicating that the domain is now predominantly filled with vapor, particularly near the outlet region.

This result is consistent with the previous Volume of Fluid (VOF) contour plot, which showed that vapor occupies the majority of the upper section. The data confirms that the reboiler is operating effectively, achieving a very high vapor quality by converting the incoming liquid into vapor.

4.2 Case 2 (Kettle Diameter 1750mm):

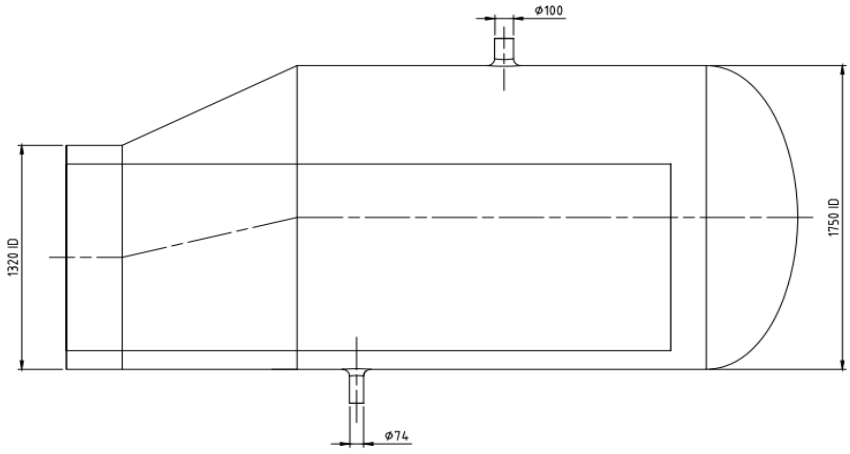

Fig 4.7: 2d Drawing of Kettle Reboiler with 1750mm Diameter

4.2.1 Effect on Pressure:

The system shown in Fig-4.8

Subcooled liquid enters under high pressure Boils inside the vessel

Vapor rises and exits at low pressure

The pressure gradient is smooth and physically consistent, indicating numerical stability and good mesh quality

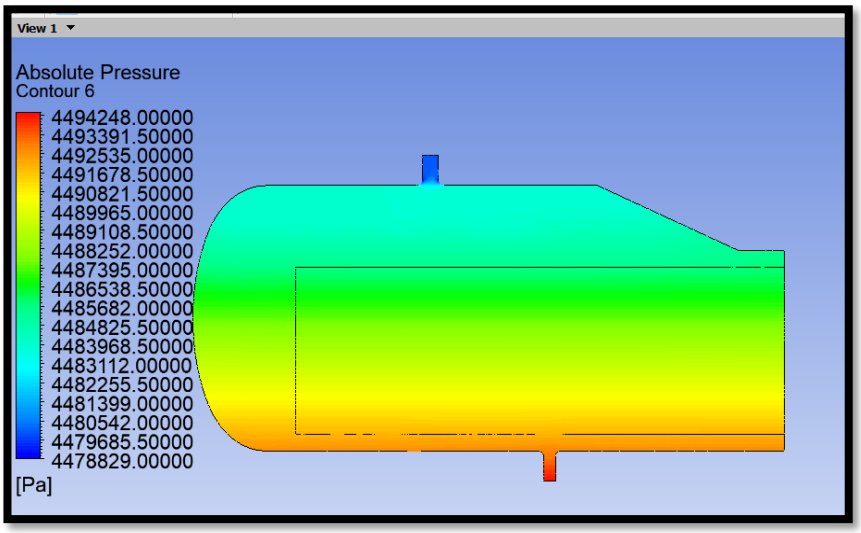

Fig. 4.8: Effect on Pressure

4.2.2 Effect on Temperature:

Subcooled liquid enters, absorbs heat, boils, and exits as superheated steam

Temperature stratification and distribution is physically accurate

Interface between liquid and vapor zones is clear and realistic in Fig-4.9

Top region holds stable superheated vapor, confirming effective phase separation

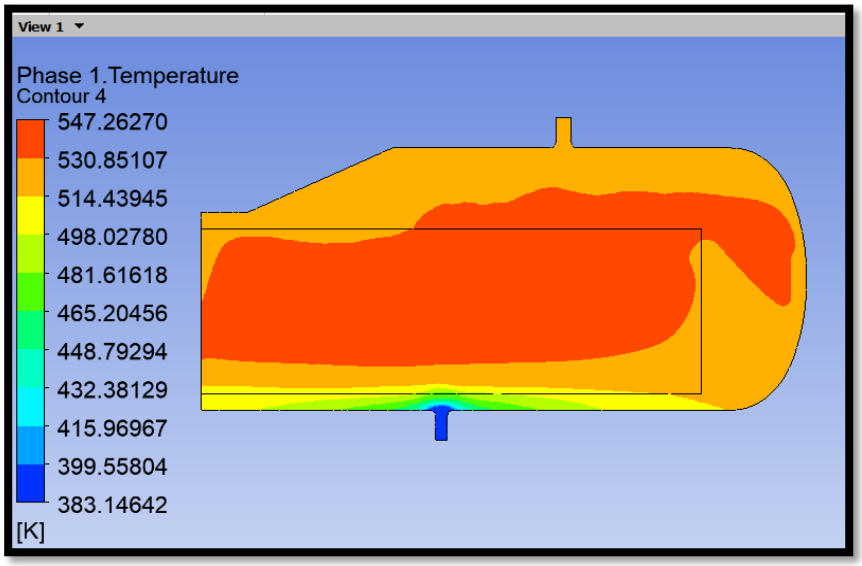

Fig. 4.9: Effect on Pressure

4.2.3 Effect on Density:

Liquid water enters from the bottom, heats up in the lower region (orange/yellow)

Boiling occurs in the mid-layers (green-yellow) in Fig 4.10

Steam rises due to buoyancy and collects at the top (blue region)

The flow develops clear thermal and density stratification inside the vessel

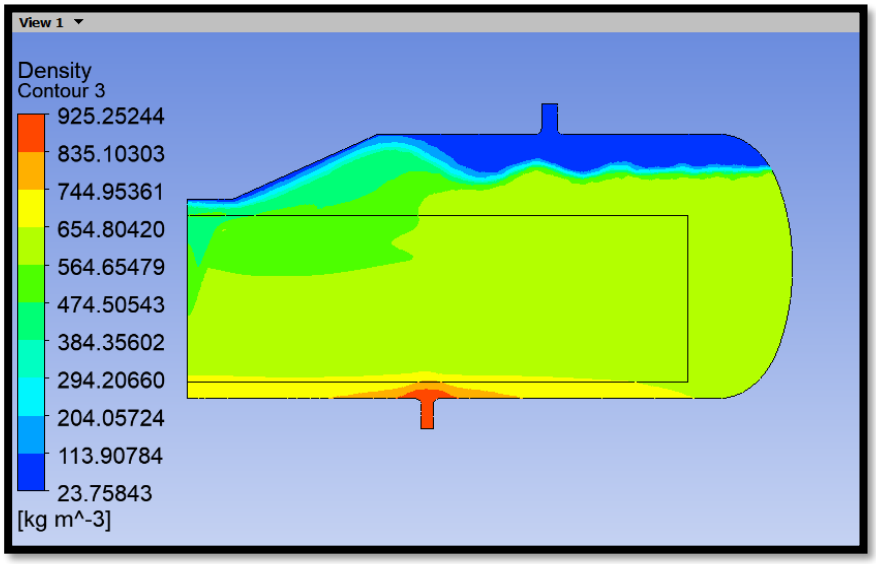

Fig. 4.10: Effect on Pressure

4.2.4 Effect on Vapor Fraction of Phase-2(vapor):

Inlet at the bottom: Subcooled/ saturated liquid enters (blue zone)

Heat transfer in the lower shell/tube region causes boiling (green/yellow). Vapor rises due to buoyancy, forming a vapor-liquid

Vapor accumulates at the top dome and exits at high quality

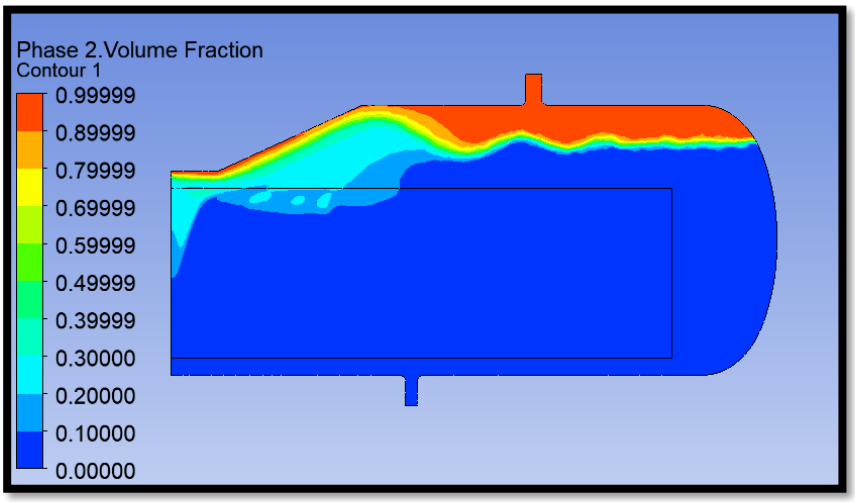

Fig. 4.11: Effect on Vapor Fraction of Phase-2(vapor)

4.2.5: Graph of mass weighted Average of phase-2 (vapor):

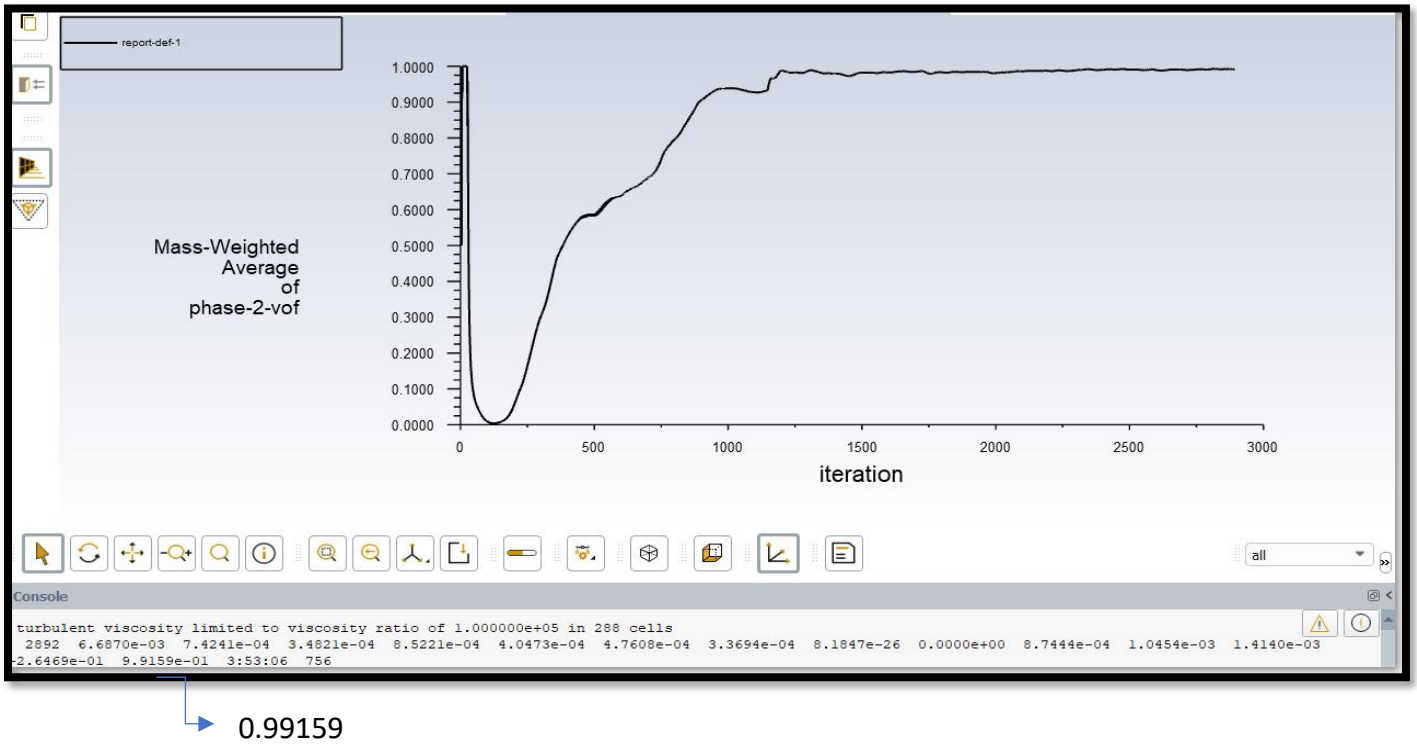

Fig. 4.12: Graph of mass-weighted Average of phase 2(vapor)

As shown in Figure 4.12, the simulation has achieved convergence for the vapor phase distribution. The final mass-weighted average vapor volume fraction (VOF for Phase-2) is approximately 0.9915. This value indicates that vapor constitutes roughly 99.15% of the total mass within the domain.

This result is consistent with the previously observed contour plot, which depicted extensive vapor regions occupying the upper section of the kettle.

4.3 Case 3 (Kettle Diameter 1690mm):

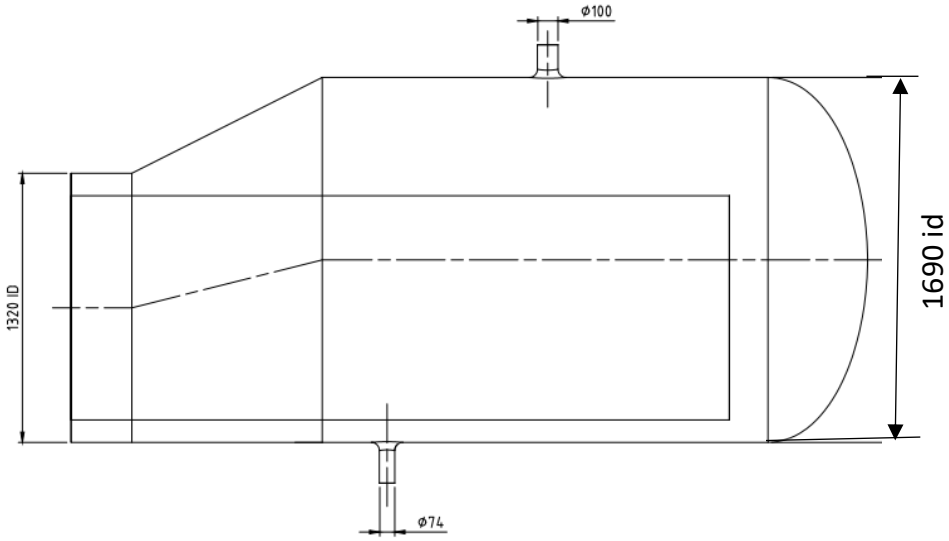

Fig. 4.13: 2d Drawing of Kettle Reboiler with 1690 mm Diameter

4.3.1 Effect on Pressure:

In Fig-4.14 Fluid enters from the bottom port (red = high pressure),

Fills the vessel, and exits from the top nozzle (blue = low pressure),

The vessel maintains a relatively uniform internal pressure, with small gradients likely due to flow friction or elevation effects.

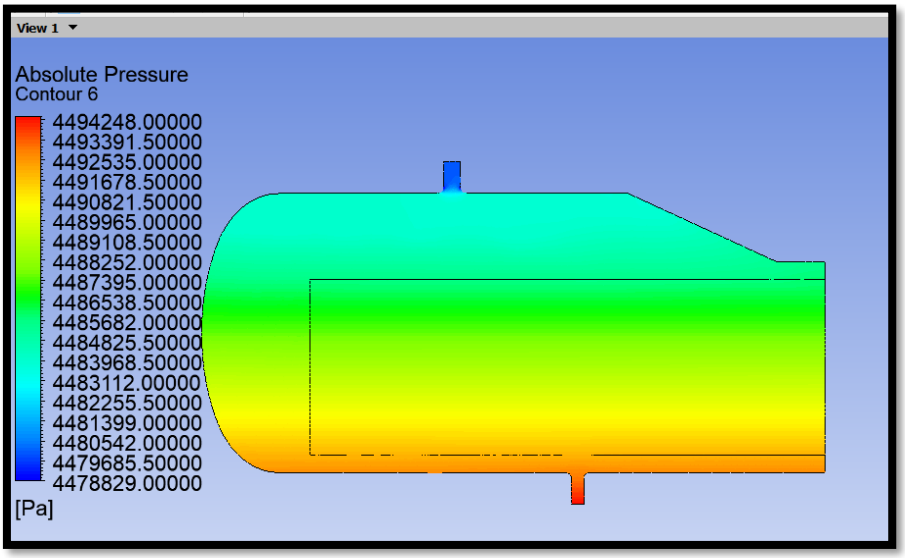

Fig. 4.14: Effect on Pressure

4.3.2 Effect on Density:

The vessel contains a multiphase fluid or gas-liquid mixture.

A heavy fluid is introduced from the bottom, and a lighter fluid exits from the top. Shown in Fig- 4 .15

There's clear density stratification, with a gradual transition zone showing partial mixing.

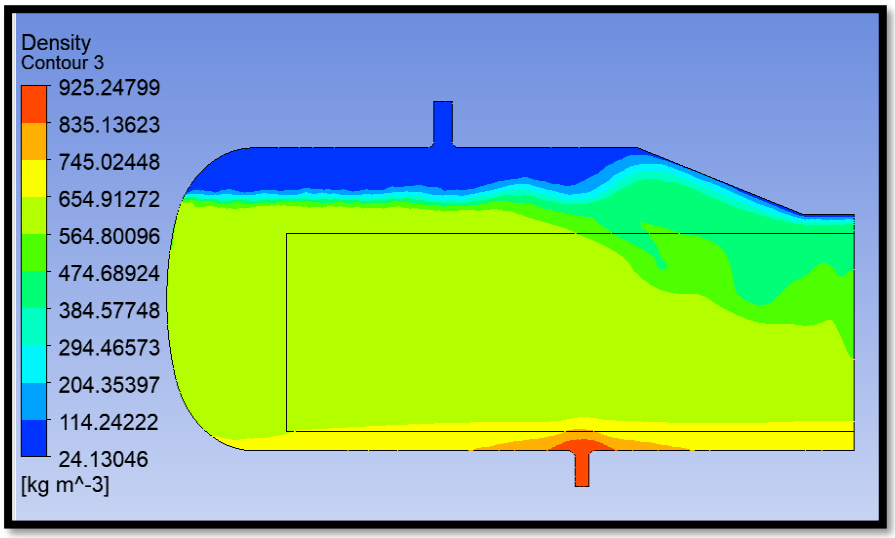

Fig. 4.15: Effect on density

4.3.3 Effect on Temperature**:**

In Fig-4.16 The simulation suggests thermal stratification, with hotter fluid accumulating at the top and cooler at the bottom. This behavior is typical in natural convection-driven systems or systems with heat sources at the top.

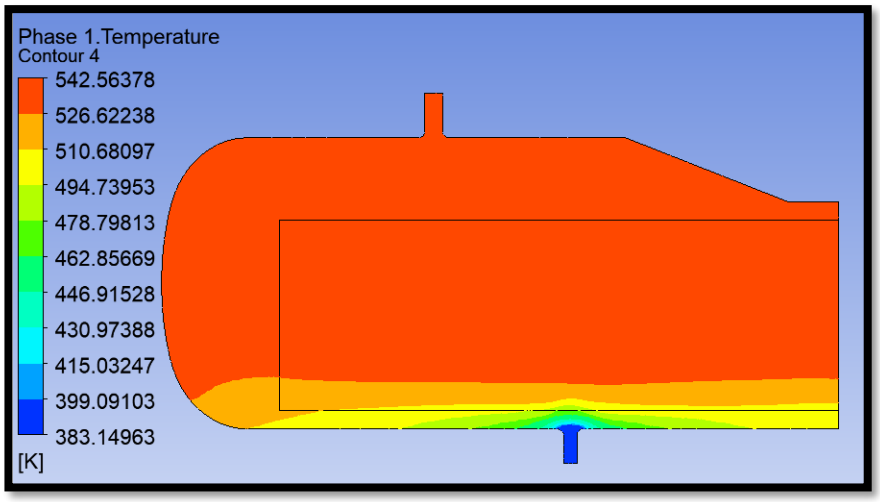

Fig. 4.16: Effect on Temperature

4.3.4 Effect on Vapor Fraction of Phase-2(vapor):

This figure-4.17 shows the local volume fraction of Phase 2, which typically means a secondary fluid phase like gas in a liquid, or vapor in liquid, or vice versa.

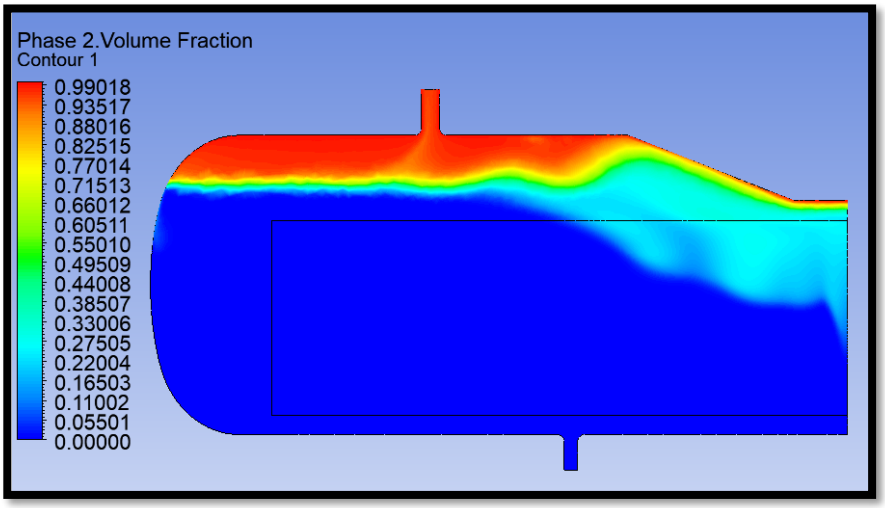

Fig. 4.17: Effect on Vapor Fraction Phase-2(vapor)

4.3.5: Graph of mass weighted Average of phase-2 (vapor):

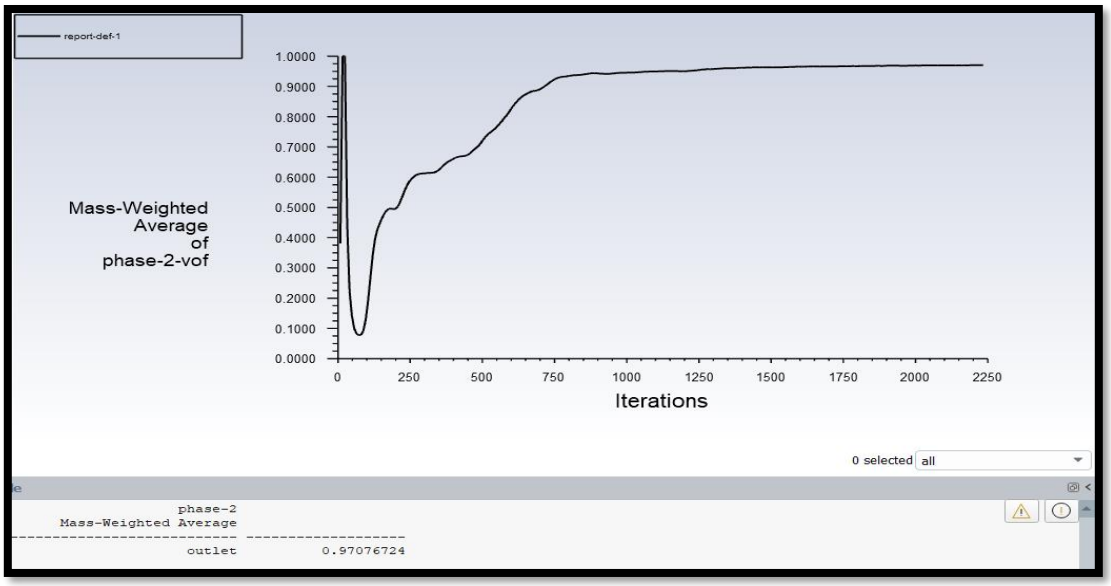

The outlet mass-weighted average Volume of Fluid (VOF) for Phase-2 is 0.9708, confirming that vapor constitutes 97.08% of the flow at the outlet. This indicates successful phase separation and a dominant presence of the vapor phase at the exit.

However, this vapor quality of 97.08% does not meet the customer's specification. A 3% liquid fraction, primarily composed of water droplets, is unacceptably high. This entrained liquid can cause significant damage to downstream equipment that utilizes this steam. Consequently, a further reduction of the kettle diameter is not feasible, as it would likely exacerbate this issue by increasing liquid carryover.

4.4 Discussion:

A comparison of both cases reveals that the vapor quality remains nearly identical. The weighted average Volume of Fluid (VOF) for Phase-2 (water vapor) is approximately 0.99 in both scenarios, as evidenced in Figures 4.6 and 4.11.

Therefore, the kettle diameter can be reduced by 40 mm without any adverse effect on system performance. This modification would yield significant material savings in the manufacturing of the kettle.

Acc to this calculation;

Decrease in diameter = 40mm

Circumference = πd

$= 3.14*40 = 125.6$ mm

$= 0.412$ ft

So, we can save up to 0.412 ft of sheet length that is used to make the kettle diameter, without any change in results or other parameters.

Based on the CFD simulation results (Figures 4.6 and 4.11), the Mass-Weighted Average of Phase-2 (water vapor) reaches approximately 0.99 in both kettle designs, indicating comparable vapor quality. Therefore, the kettle diameter can be reduced by 40 mm without compromising performance. This change results in a reduction of 125.6 mm (0.412 ft) in the sheet metal required for the kettle's circumference, contributing to material and cost savings while maintaining operational efficiency.

The current CFD analysis reveals that the outlet mass-weighted average of Phase-2 (steam) volume fraction is approximately 0.9707, indicating that around 3% of the mass flow at the outlet still consists of Phase-1 (liquid water). While this reflects a generally effective phase separation, it does not meet customer requirements for high-purity steam, as even a small percentage of entrained water can damage downstream equipment, reduce its efficiency, and lead to customer dissatisfaction. Consequently, further reducing the diameter of the kettle is not advisable, as it could increase flow velocity, reduce residence time, and exacerbate droplet carryover. To address this issue, several engineering modifications are recommended: increasing the steam space or volume to allow more time for phase separation, incorporating internal demister pads or baffles to mechanically remove entrained droplets, relocating the outlet pipe to a higher or calmer zone within the steam region, reducing inlet turbulence using diffusers or flow distributors, or adding a steam dome or dryer section to enhance droplet removal. For more accurate optimization, advanced CFD techniques such as droplet tracking or Eulerian-Lagrangian models can be employed, along with parametric studies of outlet geometry and internal design. To meet the typical industry target of 99.9% steam purity, the outlet volume fraction of -

Phase-2 should ideally be greater than 0.999, ensuring minimal moisture content and safe, efficient downstream operation.

4.5 Comparison

Table 4.1: Comparison of Parameters

Parameter:	**Case 1 (1790 mm)**	**Case 2 (1750)**	**Case 3 (1690)**
Pressure	44.8	**44.8**	44.8
Inlet water temperature	383k	**383k**	383k
Heat energy is supplied to the water	7.0440 Mega Watt	**7.0440 Mega Watt**	7.0440 Mega Watt
Vapor Fraction at outlet	0.99766	**0.99159**	0.970767

4.6 Cost Estimation:

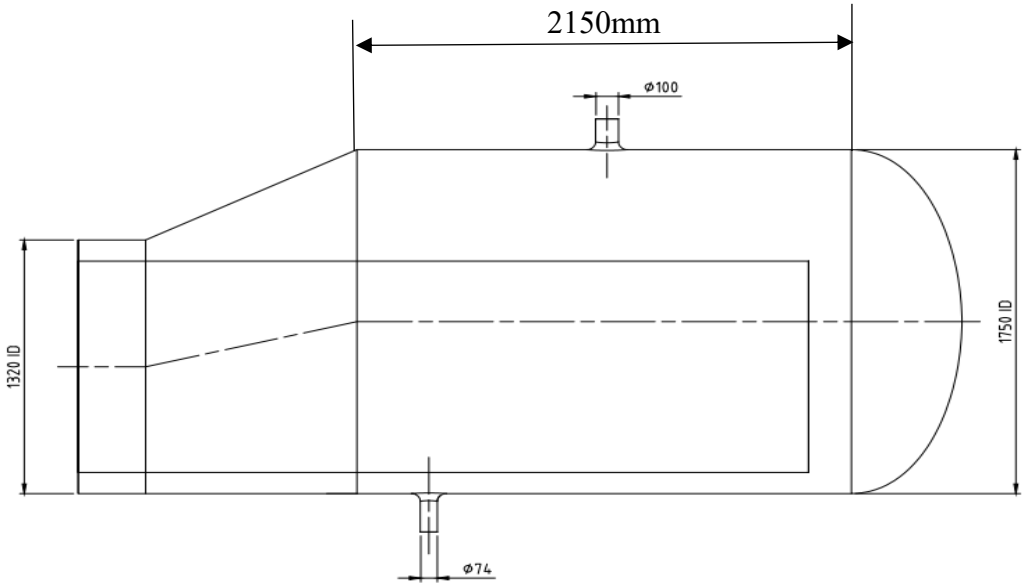

For Case 1:

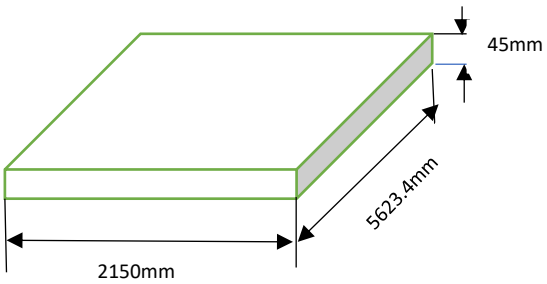

Diameter = 1790mm
Circumference = πD
= π (1790)
= 5623.4 mm
Length (L) = 2150mm
Thickness(t) = 45mm
Shell material = SA516Gr.70
SA 516 GR 70 PLATE = 60₹ (price /kg) [36]
Weight = 4379 kg
Total Price = 262740₹

For Case 2:

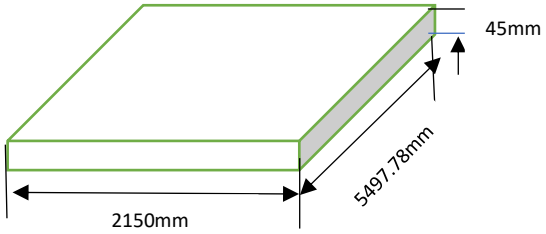

Diameter = 1750mm
Circumference = πD
= π (1750)
= 5497.78 mm
Length (L) = 2150mm
Thickness(t) = 45mm

Shell material = SA516Gr.70
SA 516 GR 70 PLATE = 60₹ (price /kg) [36]
Wight = 4276.5kg
Total Price = 256000₹

For Case 3:

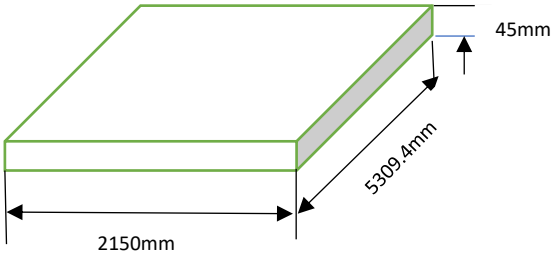

Diameter = 1690mm
Circumference = πD
= π (1690)
= 5309.4 mm
Length (L) = 2150mm
Thickness(t) = 45mm
Shell material = SA516Gr.70
SA 516 GR 70 PLATE = 60₹ (price /kg) [36]
Weight = 4129.86 kg
Total Price = 247792₹

Table 4.2: Cost comparison

Parameter:	**Case 1 (1790 mm)**	**Case 2 (1750)**	**Case 3 (1690)**
Cost ₹	262740	256000	247792

Chapter 5: Conclusion and Future Scope

5.1 Conclusion:

Based on the CFD analysis, reducing the kettle diameter by 40 mm maintains a comparable vapor quality (Phase-2 volume fraction ~0.99) without significantly affecting performance, leading to material savings (~0.412 ft of sheet metal per circumference). However, the current outlet steam purity (~97.07%) does not meet the industry standard of 99.9^{+}% or higher, as even a 3% residual liquid water content can cause downstream equipment damage, reduced thermal efficiency, and operational issues.

To achieve high-purity steam, further diameter reduction is not recommended, as it may increase flow velocity, reduce residence time, and worsen droplet carryover. Instead, design optimizations such as:

- Increasing steam space volume for better phase separation
- Adding demister pads or baffles to capture entrained droplets
- Relocating the outlet pipe to a calmer steam zone
- Reducing inlet turbulence with diffusers or flow distributors
- Incorporating a steam dome or dryer section

should be considered. Advanced CFD techniques (e.g., droplet tracking, Eulerian-Lagrangian models) and parametric studies can further refine the design for optimal performance.

- This study investigated the feasibility of reducing the kettle reboiler diameter from 1790 mm to 1750 mm while maintaining optimal vapor quality (~0.997 dryness fraction) and separation efficiency. Through ANSYS Fluent simulations

- The 40 mm reduction showed no significant impact on vapor-liquid separation, proving that material savings (0.412 ft of sheet metal per unit) can be achieved without performance loss.
- This optimization yields significant material and cost savings without performance loss

5.2 Future Scope:

1. Enhanced CFD Modeling – Implement multiphase flow tracking for precise droplet separation analysis.
2. Design Optimization Studies – Evaluate different internal geometries, baffle configurations, and outlet placements for improved steam purity.
3. Material & Cost Efficiency – Explore lightweight, corrosion-resistant materials while maintaining structural integrity.
4. Prototype Testing – Validate CFD predictions with experimental data for real-world performance.
5. Automation & Control Integration – Investigate real-time monitoring and adaptive control to maintain optimal steam quality under varying loads.

By addressing these aspects, the kettle design can achieve higher efficiency, lower costs, and compliance with stringent steam purity standards, ensuring reliable and safe operation in industrial applications.

References

[1]. R. K. Shah, "Heat Exchangers," in Encyclopedia of Energy Technology and the Environment, edited by A. Bisio and S. G. Boots, pp. 1651-1670, John Wiley & Sons, New York, 1994.

[2]. R. K. Shah and A. C. Mueller, "Heat Exchange," in Ullmann's Encyclopedia of Industrial Chemistry, Unit Operations II, Vol. B3, Chapter 2, pp. 2-1-2-108, VCH Publishers, Weinheim, Germany, 1989.

[3]. G. Walker, Industrial Heat Exchangers Basic Guide, 2d ed., Hemisphere, Washington, DC, 1990.

[4]. G. E Hewitt, coordinating ed., Hemisphere Handbook of Heat Exchanger Design, Hemisphere, Washington, DC, 1989.

[5]. Tubular Exchanger Manufacturers Association, Standards of TEMA, 7th ed., New York, 1988.

[6]. K. K. Shankar Narayanan, Plate Heat Exchangers, Proc. Symposium on Heat Exchangers, Paper IT-3, Indira Gandhi Centre for Atomic Research, Kalpakkam 603102, India, February 1996.

[7] R. K. Shah and A. C. Mueller, "Heat Exchanger Basic Thermal Design Methods," in Handbook of Heat Transfer Applications, 2d ed., W. M. Rohsenow, J. E Hartnett, and E. N. Gani~ (eds.), Chapter 4, Part 1, pp. 1-77, 1985.

[8] Mechanical engineers handbook: energy and power / edited by Myer Kutz. – Fourth edition.

[9] J.W. Palen, “Shell and Tube Reboilers,” Section 3.6, HEDH.

[10] Palen J. W. Shell-and-tube reboilers. In: Heat Exchanger Design Handbook, Vol. 3. New York: Hemisphere Publishing Corp.; 1988.

[11] Kister HZ. Distillation Operation. New York: McGraw-Hill, 1990.

[12] Alon Davidy, “CFD Simulation of Forced Recirculating Fired Heated Reboilers,” 2020.

[13] B.M. Burnside, “2-D kettle Reboiler circulation model” International Journal of Heat and Fluid Flow; 1999.

[14]; “Design and Analysis for the Improvement of Electric Kettle Performance”

[15] Husam J. Alsaemre, Adnan A. Ateeq, Ali N. Kalaf; “Optimum Design Parameters with the Lowest Cost of Basra Refinery Kettle Reboiler” EAI. 2022.

[16] Gianluca Rossiello, Muhammad Ali Uzair, Seyed ¨Integrated use of CFD and field data for accurate thermal analyses of oil/gas boilers” 2023

[17] R. Mukherjee; “Practical Thermal Design of Shell-and-Tube Heat Exchangers”; 2004

[18] Sloley AW. Properly design thermosyphon reboilers. Chem Eng Prog 1997;93(No. 3):52–64.

[19] Kister HZ. Distillation Operation. New York: McGraw-Hill, 1990.

[20] Fair JR. Vaporizer and reboiler design: Part 1. Chem Eng 1963;70(No. 14):119–24.

[21] Palen JW, Small WM. A new way to design a kettle and internal reboilers. Hydrocarbon Proc 1964;43(No. 11):199–208.

[22] Bell KJ, Mueller AJ. Wolverine Engineering Data Book II. Wolverine Tube, Inc., www.wlv.com; 2001.

[23] Shinskey FG. Distillation Control. New York: McGraw-Hill, 1977.

[24] Thome JR. Engineering Data Book III. Wolverine Tube, Inc., www.wlv.com; 2004.

[25] Lee DC, Dorsey JW, Moore GZ, Mayfield FD. Design data for thermosyphon reboilers. Chem Eng Prog 1956;52(No. 4):,160–164.

[26] Dowlati R, Kawaji M. Two-phase flow and boiling heat transfer in tube bundles, Chapter 12. In: Kandlikar SG, Shoji M, Dhir VK, editors. Handbook of Phase Change: Boiling and Condensation. Philadelphia, PA: Taylor and Francis; 1999.

[27] Fair JR. What you need to design thermosyphon reboilers. Pet Refiner 1960;39(No. 2):105–23.

[28] Fair JR, Klip A. Thermal design of horizontal reboilers. Chem Eng Prog 1983;79(No. 3):86–96.

[29] Yilmaz SB. Horizontal shell side thermosyphon reboilers. Chem Eng Prog 1987;83(No. 11):64–70. [14] Hewitt GF, Shires GL, Bott TR. Process Heat Transfer. Boca Raton, FL: CRC Press; 1994.

[30] Collins GK. Horizontal thermosyphon reboiler design. Chem Eng 1976;83(No. 15):149–52.

[31] Palen JW, Shih CC, Taborek J. Mist flow in thermosyphon reboilers. Chem Eng Prog 1982;78(No. 7):59–61.

[32] Anderson, John David, and John Wendt. *Computational fluid dynamics*. Vol. 206. New York: McGraw-Hill, 1995.

[33] Palen JW, Johnson DL. Evolution of kettle reboiler design methods and present status, Paper No. 13i. Houston: AIChE National Meeting; March 14–18, 1999.

[34] Perry RH, Chilton CH, editors. Chemical Engineers' Handbook. 5th ed. New York: McGraw-Hill, 1973.

[35] Anderson, John David, and John Wendt. *Computational fluid dynamics*. Vol. 206. New York: McGraw-Hill, 1995.

[36] https://www.unisteelsengg.com/SA-516-GR-70-PLATE-sheet-plate.html (7/30/2025- 10:30)

[37] Shih, T.-H. et al. (1995). "A New k-ε Eddy Viscosity Model..." Computers & Fluids, 24(3), 227-238.